Research Square

Preprints are preliminary reports that have not undergone peer review.
They should not be considered conclusive, used to inform clinical practice,
or referenced by the media as validated information.

Sustainable Utilization of Bayer Process Red Mud in Subgrade Engineering: A Comprehensive Review on Multi-Scenario Applications, Mechanical Performance, and Environmental Implications

Bo YANG

doctoryang@zohomail.cn

Henan Province Key Laboratory of Recycling of Solid Waste Material for Road Engineering

Xiaofeng WANG

Henan Province Key Laboratory of Recycling of Solid Waste Material for Road Engineering

Jianfei LIU

Henan Zhonggong Design & Research Group CO., LTD

Xiaoguo ZHANG

Henan Zhonggong Design & Research Group CO., LTD

Chenguang WAN

Henan Zhonggong Design & Research Group CO., LTD

Systematic Review

Keywords: Bayer Process Red Mud (BPRM), highway subgrade engineering, soil stabilization, mechanical performance, environmental safety

Posted Date: November 3rd, 2026

DOI: https://doi.org/10.21203/rs.3.rs-11257627/v1

License: This work is licensed under a Creative Commons Attribution 4.0 International License.
Read Full License

Additional Declarations: No competing interests reported.

Sustainable Utilization of Bayer Process Red Mud in Subgrade Engineering: A Comprehensive Review on Multi-Scenario Applications, Mechanical Performance, and Environmental Implications

Abstract

The disposal of Bayer process red mud (BPRM), a major solid waste from alumina production, is a long-standing environmental concern owing to its high alkalinity and potential for contaminant leaching. While various resource recovery strategies have been explored, its comprehensive utilization rate remains disappointingly low, impeding the green transformation of the aluminum industry. Highway engineering offers a practical solution for its bulk consumption, primarily through two approaches: replacing conventional soil fills in subgrades and enhancing soil properties as a stabilization agent. Recent research has systematically demonstrated the feasibility of these applications, leading to several successful full-scale projects. This paper provides a comprehensive review of this field. It begins by characterizing the properties of BPRM, followed by a detailed discussion on the mechanisms, technical performance, engineering applications, and environmental impacts of various red mud-based subgrade materials, including modified red mud, red mud-based foamed lightweight soil, and red mud-stabilized soil. The review concludes by highlighting the current challenges and proposing future research avenues to advance the resource utilization of red mud in subgrade engineering.

Keywords: Bayer Process Red Mud (BPRM), highway subgrade engineering, soil stabilization, mechanical performance, environmental safety

1. Introduction

Aluminum serves as a critical fundamental material underpinning national economic development, strategic emerging industries, and the modernization of defense-related science and technology. Owing to its advantageous properties, it is extensively employed across diverse sectors, including construction, packaging, transportation, power generation, and aerospace. As China's industrialization accelerates, both the domestic demand for and production of aluminum have exhibited sustained growth. According to data released by the International Aluminium Institute and the National Bureau of Statistics of China, the nation's primary aluminum (electrolytic aluminum) output reached 45.02 million tonnes in 2025, accounting for over 60% of the global total (Fig1).

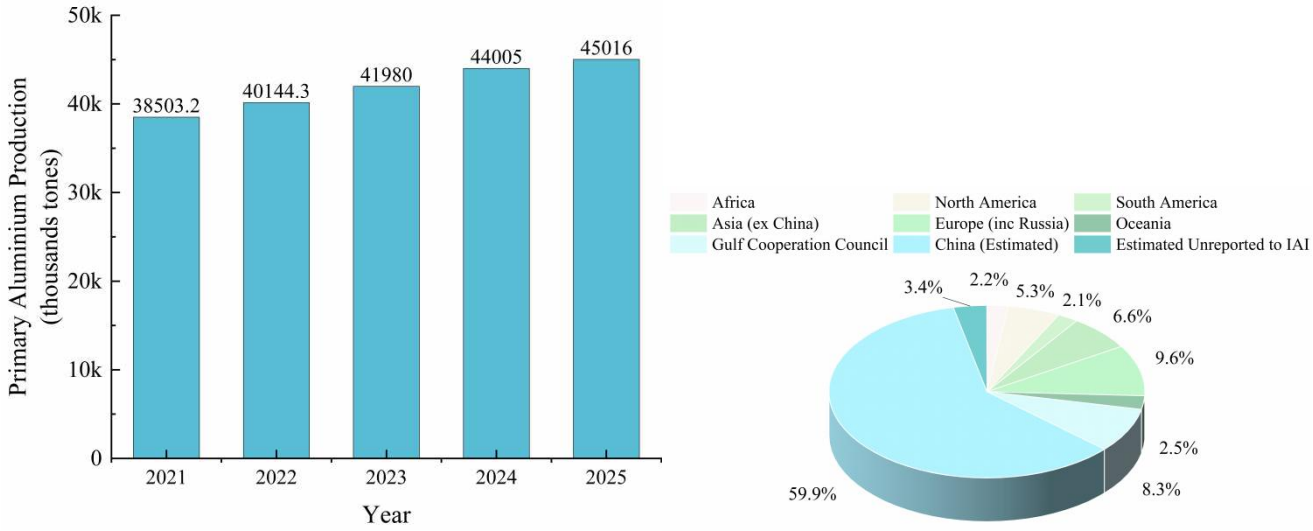


Fig.1 Primary aluminium production

The rapid expansion of the aluminum industry has raised considerable environmental concerns, particularly in relation to the generation and management of red mud, a highly alkaline solid waste produced during alumina extraction from bauxite. This extraction process is a key step in the production of primary (electrolytic) aluminum and is predominantly carried out using the Bayer process [1–3] . For every metric ton of aluminum produced, approximately 2.0 to 3.2 metric tons of red mud are generated [4–7] .

Bayer process red mud(BPRM) is characterized by its high pH, elevated salinity, and fine particle size, which collectively hinder its large-scale valorization. As a result, red mud is primarily managed through on-site impoundment using dam structures. Wet-stacked red mud contains substantial quantities of caustic liquor, which poses a serious risk of leachate migration into surface and groundwater systems, potentially disrupting aquatic ecosystems. In contrast, dry-stacked red mud is prone to wind erosion due to its fine and desiccated nature, leading to fugitive dust emissions. These airborne particulates can contribute to ambient air pollution and facilitate the dispersion of alkaline substances and trace metals, resulting in soil degradation and vegetation stress in

surrounding areas. In some areas, residential areas and farmlands are distributed in the vicinity of red mud stockpiles, which further exacerbate the environmental risks (Fig.1). Such environmental risks underscore the urgent need for sustainable red mud management strategies and mitigation measures [8–12] .



Fig.2 Red mud stockpile together with surrounding residential areas and farmlands

In response to the significant environmental challenges associated with the stockpiling of BPRM, extensive efforts have been made in recent years to explore its safe and comprehensive utilization. Currently, BPRM has been investigated as a secondary resource for the recovery of valuable components such as Al_2O_3, Fe_2O_3, TiO_2, and a range of rare and trace metals [13–16]. In addition, it has found potential applications in the production of cement clinker and red mud bricks for use as construction materials [17–22] . BPRM has also been utilized as an alkaline activator for the synthesis of geopolymer materials [23–29], and as a functional material for the adsorption of pollutants from wastewater and the remediation of acidic soils [30–37]. These diverse utilization pathways offer promising avenues for mitigating the environmental burden posed by red mud disposal.

Although BPRM has demonstrated feasibility in multiple valorization pathways, its comprehensive utilization remains limited in scale. In 2023, China generated 107 million tons of red mud, with only over 10 million tons utilized, resulting in a utilization rate of merely 9.8%. Globally, red mud valorization rates do not exceed 15% [14, 38]. As a resource-intensive sector, highway engineering requires large-scale material consumption. Subgrade construction for standard four-lane expressways in China's plains and hilly regions consumes approximately 130,000 m^3 of soil per kilometer. Employing red mud as replacement fill or stabilization material through waste-based soil replacement and waste-based soil stabilization strategies offers dual benefits: mitigating environmental contamination while addressing infrastructure material deficits. This approach aligns with green

development objectives by diverting industrial waste streams, thereby advancing resource sustainability with significant scalability potential.

The utilization of red mud in subgrade engineering has garnered substantial research attention, with numerous studies exploring its potential as a substitute for subgrade soil and in the development of red mud-based cementitious materials for soil improvement [11, 39–47]. Notable engineering implementations have validated the feasibility of recycling BPRM in subgrade applications [5, 40]. While existing literature has extensively documented the resource utilization of BPRM, these studies predominantly focus on single-material modification or specific application scenarios, thereby lacking a systematic overview of its multi-scenario resource utilization in subgrade engineering.

Several reviews have already addressed red mud in road engineering. Mukiza et al. [49] surveyed the use of red mud in road base and subbase courses, concentrating on the strength-formation mechanism and leaching of a single red-mud-based road base system, whereas Singh et al. [45] reported experimental investigations of red mud as a road construction material and Silveira et al. [48] reviewed construction applications of red mud more broadly while giving limited attention to subgrade mechanics and in-service leaching; Jia et al. [9] reviewed engineered treatments of red mud, including construction materials and metal recovery. None of these integrates the three parallel material families treated here, namely replacement fills, composite-modified red mud, and red-mud-based foamed lightweight soil, nor compares them on a common set of mechanical, stiffness-related and environmental indicators. The present review therefore treats replacement and stabilisation as two distinct design logics rather than one, consolidates the coupled mechanisms governing composite modification into a single framework, and traces the environmental evidence from static batch leaching through dynamic column tests to coupled modelling and field monitoring.

This review aims to systematically summarize the current status of BPRM resource utilization in subgrade engineering, encompassing its application as a substitute for subgrade soil and in the stabilization of various engineered soils. It investigates the underlying mechanisms and technical performance of BPRM under different subgrade engineering contexts, evaluates the environmental risks associated with its application, reviews international case studies of BPRM in subgrade projects, and outlines future research directions. The overarching objective is to broaden the engineering applications of BPRM and facilitate its large-scale sustainable implementation for waste reduction.

2. Systematic Review Methodology

2.1. Literature Search Strategy

A comprehensive literature search was conducted across four core academic databases: Web of Science, Scopus, ScienceDirect, and OpenAlex. The search period was set from January 2016 to July 2026, to cover the latest research progress in the field over the past 10 years. The Boolean search string used was:

("Bayer red mud" OR "red mud" OR "Bayer process red mud") AND ("road subgrade" OR "highway subgrade" OR "road embankment" OR "subgrade fill" OR "pavement subgrade" OR "subgrade material" OR "soil stabilization" OR "soil improvement" OR "road foundation")

2.2. Inclusion and Exclusion Criteria

To ensure the relevance and quality of the included literature, the following inclusion and exclusion criteria were established:

Inclusion Criteria: (1) Peer-reviewed journal articles, review papers, and conference proceedings; (2) Research focusing on Bayer process red mud (excluding sintering process red mud); (3) Research related to highway subgrade engineering scenarios (embankment fill, subgrade bed, subgrade soil stabilization); (4) Research reporting material properties, modification mechanisms, mechanical performance, engineering applications, or environmental safety of BPRM.

Exclusion Criteria: (1) Research focusing on non-Bayer process red mud; (2) Research focusing on pavement surface, base, or subbase layers (excluding subgrade); (3) Non-road application scenarios (e.g., building materials, wastewater treatment, metal recovery); (4) Duplicate publications, abstract-only papers, book chapters, and patent documents.

According to the inclusion and exclusion criteria above, a total of 220 relevant literatures were retrieved, their detailed distribution were presented as Fig3.

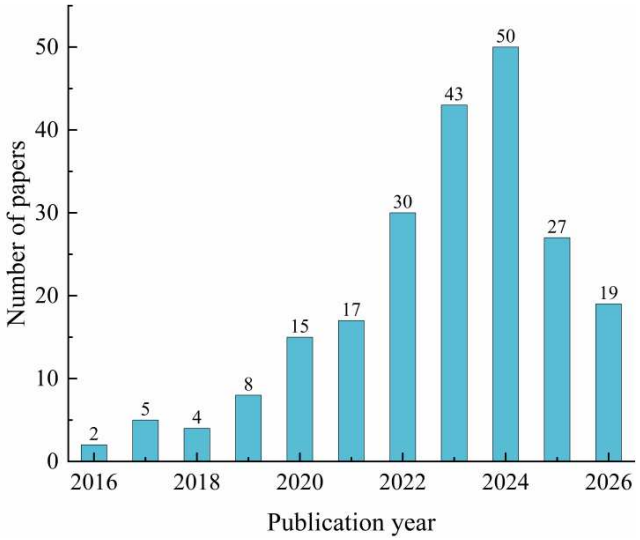


Fig.3 Relevant literatures distribution

3. Fundamental Properties of BPRM

3.1. Generation process of BPRM

Red mud is the primary solid waste produced by the alumina industry. The alumina production processes fall into four categories: alkaline, acid, combined acid-base, and thermal methods. The industrial production mainly uses alkaline methods, which primarily include the Bayer process and the sintering process [21, 38, 48]. Characterized by its simple flowsheet, operational convenience, and high-quality output, the Bayer process is adopted by approximately 95% of global enterprises for alumina extraction [2, 6, 49]. This process is suitable for refining high-grade bauxite with a silica ratio ranging from 7 to 10 [50]. The fundamental principles of the Bayer process involve three sequential steps: extraction, precipitation, and sintering:

Extraction: Under conditions of elevated temperature and pressure, aluminum hydroxide in bauxite reacts with sodium hydroxide to produce a soluble sodium aluminate solution.

$$Al(OH)_3(s) + NaOH(aq) \rightarrow Na^+ + Al(OH)_4^-(aq) \quad (1)$$

$$AlO(OH)(s) + NaOH(aq) + H_2O \rightarrow Na^+ + Al(OH)_4^-(aq) \quad (2)$$

Precipitation: The sodium aluminate solution resulting from leaching is diluted and cooled, after which aluminum hydroxide seed crystals are added. The alumina in the solution progressively precipitates, forming aluminum hydroxide precipitates.

$$Na^+ + Al(OH)_4^-(aq) \rightarrow Al(OH)_3(s) + NaOH(aq) \quad (3)$$

Sintering: The washed and filtered aluminum hydroxide is calcined at temperatures above 1000°C to remove crystalline water, ultimately yielding the alumina product.

$$2Al(OH)_3(s) \rightarrow Al_2O_3(s) + 3H_2O(g) \quad (4)$$

The Bayer process typically uses a concentrated sodium hydroxide solution to convert aluminum hydroxide into sodium aluminate. By diluting the solution and adding aluminum hydroxide seed crystals, aluminum hydroxide is re-precipitated, and the remaining sodium hydroxide solution is recycled for subsequent bauxite processing, facilitating continuous production. The main process flow (Fig. 4) comprises: raw pulp preparation, high-pressure leaching, dilution of the pressurized leaching slurry and red mud separation/washing, seed decomposition, classification/washing of aluminum hydroxide, calcination of aluminum hydroxide, and mother liquor evaporation. During the leaching process, oxides of iron, silicon, and titanium in bauxite partially remain unreacted in the solid phase. These residues, after precipitation and filtration, form red mud.

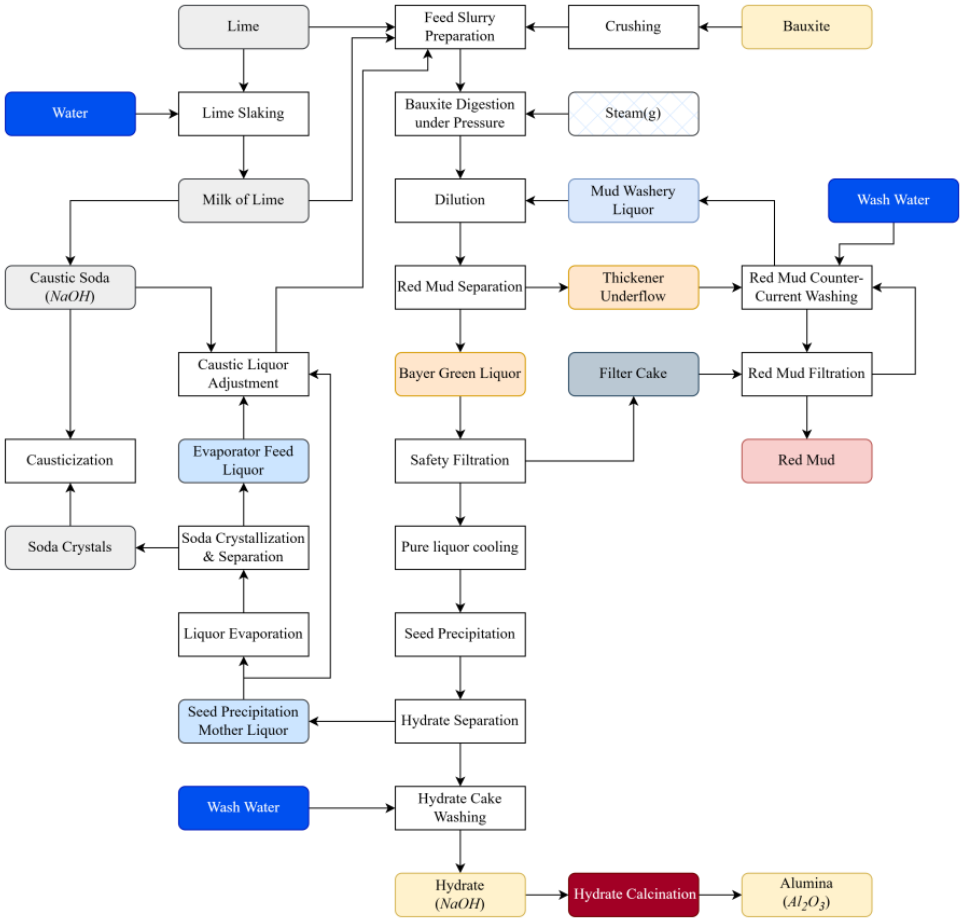


Fig.4 Schematic diagram of Bayer process production process

3.2. Chemical Characteristics of BPRM

The chemical composition of red mud from the Bayer process comprises Al_2O_3, Fe_2O_3, CaO, SiO_2, Na_2O, among others, and the concentrations of these components are significantly influenced by factors including the origin of the bauxite, the processing technology, and the duration of stacking [6, 51–53]. Based on publicly available data from domestic literature and the sampling analysis of BPRM conducted by the authors at Chinalco Zhongzhou Aluminum Co., Ltd. (located in Xiuwu County, Henan Province), the chemical composition of BPRM is primarily dominated by Fe_2O_3, Al_2O_3, and SiO_2 (Table 1). Although it contains a considerable amount of silicon and aluminum components, most of these elements exist in the form of stable aluminosilicates, resulting in low reactivity [17, 54]. The content of Fe_2O_3 in BPRM can reach up to 50% (Fig.5), hence its overall appearance is characterized by a reddish-brown color (Fig. 6).

Table 1 Main chemical components of BPRM in China

Source location	Al_2O_3	Fe_2O_3	SiO_2	CaO	TiO_2	Na_2O	References
Zouping, Shandong	19.9	51.1	10.4	1.3	8.9	7.4	[55]

Zibo, Shandong	21.4	34.3	20.1	3.2	2.0	8.1	[56]
Binzhou, Shandong	21.9	22.7	18.6	11.7	7.1	10.2	[57]
Xingyang, Henan	24.5	10.9	21.6	15.8	2.3	7.4	[58]
Taiyuan, Shanxi	24.3	9.4	20.2	18.3	/	9.6	[59]
Qingzhen, Guizhou	13.7	14.4	18.6	31.1	4.8	13.4	[56]
Baise, Guangxi	21.6	29.5	15.1	11.5	5.6	9.2	[42]
Sp., Henan	3.32	20.1	13.3	32.0	3.8	10.9	[60]
Yantai, Shangdong	27.8	35.8	15.1	1.9	6.0	12.0	[61]
Gongyi, Henan	20.9	26.1	27.3	8.2	/	9.6	[62]
Zibo, Shandong	17.9	33.9	19.4	2.7	/	12.2	[63]
Liaocheng, Shangdong	26.3	35.4	17.5	1.4	/	12.9	[64]
Xiuwu, Henan	20.2	31.6	24.3	3.0	3.4	5.1	/

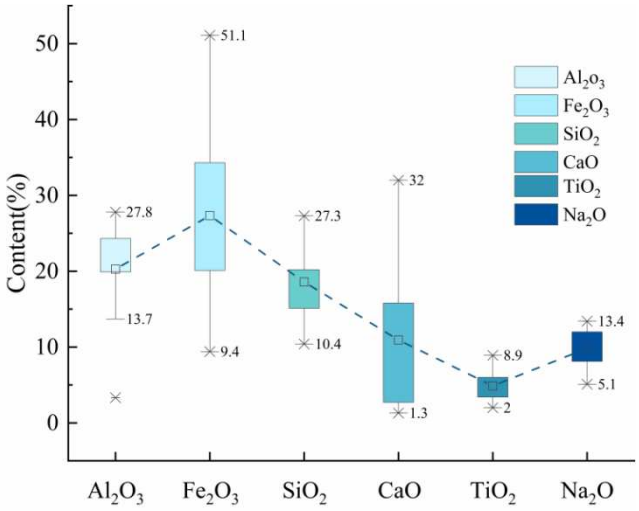


Fig.5 Chemical components content of BPRM



Fig.6 Appearance of BPRM (Photo taken at the storage yard of Chalco Zhongzhou Aluminum Co., Ltd.)

The alkalinity of BPRM is an intrinsic inheritance of the digestion chemistry rather than a property of the bauxite itself. During Bayer processing, concentrated *NaOH* liquor dissolves the aluminium-bearing phases of the ore, and the sodium that is not recovered with the pregnant liquor is discharged with the residue, so that BPRM typically carries 2-10 wt.% Na_2O, with values of 6.79 wt.% Na_2O and 1.37 wt.% K_2O reported for a representative Chinese refinery residue [65]. Contemporary reviews consistently partition this alkali into two chemically distinct reservoirs: soluble free alkali (SFA) and chemically bound alkali (CBA) [66, 67].

The SFA originates from the caustic liquor entrained in the residue pore space that cannot be fully recovered by counter-current decantation washing; it comprises *NaOH*, $NaAl(OH)_4$, Na_2CO_3, $NaHCO_3$ and Na_2SiO_3, together with minor *KOH* and K_2CO_3, and accounts for only about 20-25 % of the total alkali [67–70]. Under evaporative conditions, these alkalis readily migrate to the material's surface, inducing the phenomenon of efflorescence [71] (Fig. 7).



Fig.7 BPRM surface "efflorescence" phenomenon (photo taken at the storage yard of Henan Baiaoheng New Material Technology Co., Ltd.)

The CBA accounts for about 75-80% of the total alkali, which is structurally incorporated in the desilication products, principally sodalite ($[Na_6Al_6Si_6O_{24}]\cdot[2NaX\ or\ Na_2X]$, X = OH^-, CO_3^{2-}, Cl^-, SO_4^{2-}) and cancrinite ($[Na_6Al_6Si_6O_{24}]\cdot 2CaCO_3$), accompanied by calcium-bearing alkaline phases such as tricalcium aluminate ($Ca_3Al_2(OH)_{12}$), hydrogarnet ($Ca_3Al_2(SiO_4)_x(OH)_{12-4x}$) and calcite [67, 72].

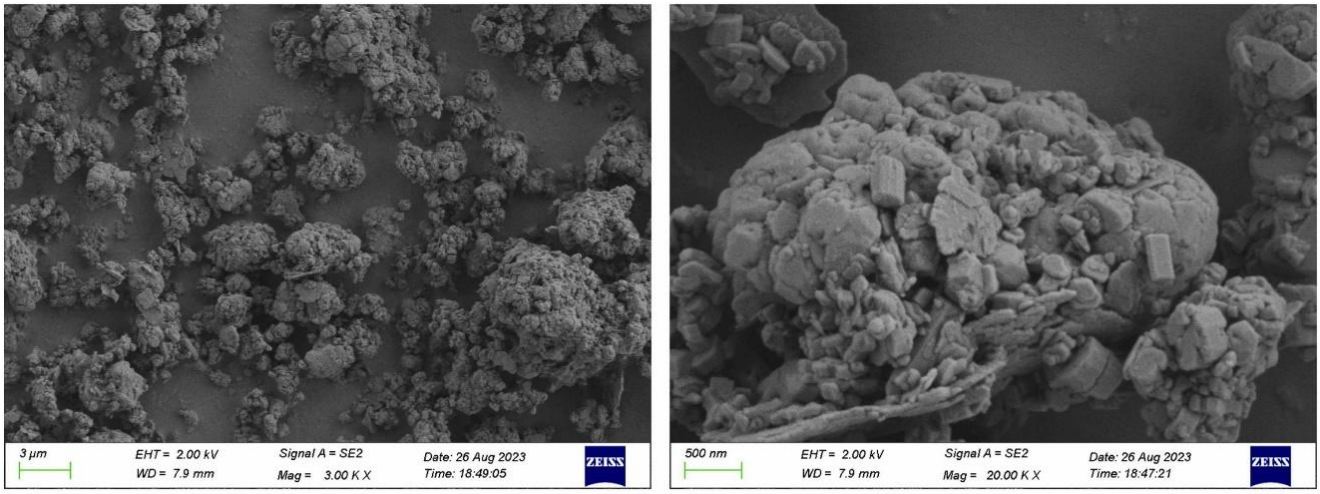
The fresh BPRM reports high pH value of 10-13 [3, 4, 69, 73–75], the initial pH value is set by instantaneous dissolution of the SFA, which releases OH^-, CO_3^{2-}, $Al(OH)_4^-$ and SiO_3^{2-}. During long-term service, following mineralization and precipitation reactions, alkaline mineral phases such as sodalite, cancrinite, hydrogarnet, and calcite undergo partial dissolution, establishing a dissolution equilibrium. This process stabilizes the concentration of alkaline anions (e.g., OH^-, CO_3^{2-}) in the solution [66, 69], maintaining the high pH value of BPRM.

3.3. Engineering Characteristics of BPRM

3.3.1. Particle Characteristics

After undergoing processes such as grinding and filtering, the particles of BPRM are relatively fine. At the microscopic level, scanning electron microscopy (SEM) images of BPRM display numerous micrometer-scale fine particles (Fig. 8a), which aggregate into loose, porous macroparticles with rough surfaces (Fig. 8b) [54]. Consequently, BPRM has a high specific surface

area, typically ranging from 64 to 186 m^2/g [76], which is significantly higher than that of limestone powder at similar particle sizes [50]. At the macroscopic level, the fine fraction, which includes particles smaller than 0.075 mm (consisting of silt and clay), constitutes over 90% of the BPRM [4, 54, 77], classifying it as a typical fine-grained soil. Due to variations in bauxite grinding, processing conditions, and hydrodynamic forces during wet disposal, the proportions of silt and clay differ: some samples are dominated by silt [4], resembling silty soil, while others are rich in clay [56], resembling clayey soil.



(a)

(b)

Fig.8 SEM Microscopic morphology of BPRM particles[54] (a)3 000× (b)20 000×

3.3.2. Natural Moisture Content

In the production of alumina, bauxite is subjected to high-pressure digestion and subsequent processes, which yield a slurry consisting of a sodium aluminate solution and red mud. Traditionally, BPRM is primarily disposed of using the wet disposal method, and the fine particles carry a net negative surface charge and are strongly hydrophilic, so a thick adsorbed water film persists even after pressure filtration and the as-discharged mud retains a natural moisture content ranging from 35% to 45%, sometimes it can be as high as nearly 50% [40, 56, 78]. In recent years, regions such as Guizhou and Shanxi have updated traditional wet disposal methods by integrating filtration and dewatering processes. This has significantly reduced the water content of BPRM to below 30%. As a result, this advancement facilitates dry disposal of red mud, thereby mitigating environmental pollution and decreasing the land required for storage.

3.3.3. Boundary Water Content and Classification of Fine-Grained Soil

Based on data from published literature, BPRM typically exhibits a liquid limit ranging from 40% to 60% and a plastic limit between 30% and 40%, both of which are relatively high. Its plasticity index is generally less than 17, commonly falling within 10 to 16 [56, 58, 78]. According to the provisions for soil classification specified in the Chinese standard “Test Methods of Soils for Highway Engineering” (JTG 3430-2020), the plasticity index of red mud predominantly plots below the A-line on the plasticity

chart. This indicates characteristics more akin to silt (Table 2).

Table 2 Limit moisture content and classification of fine grained soil of BPRM

Source Location	Liquid Limit (%)	Plastic Limit (%)	Plasticity Index	Classification of Fine-Grained Soils	References
Zhengzhou, Henan	48.2	36.5	11.7	ML	[58]
Qingzhen, Guizhou	50.0	34.7	15.3	MH	[56]
Qingzhen, Guizhou	49.6	35.3	14.3	ML	[56]
Qingzhen, Guizhou	49.8	34.6	15.3	ML	[56]
Zibo, Shandong	58.5	42.1	16.4	MH	[78]
Binzhou, Shandong	51.4	36.1	15.3	MH	[78]
Sp., Henan	50.2	33.8	10.4	MH	[60]

4. Waste-for-Soil Replacement: BPRM as Sustainable Subgrade Fill Material

The engineering properties of BPRM resemble those of silt, characterized by high natural moisture content, high liquid limit, low strength, and poor water stability. Consequently, it is generally unsuitable for direct use as subgrade fill material [40, 79, 80]. A common method involves using BPRM as the main filling material, which must constitute at least 50% by mass, while incorporating other materials to improve its technical properties, thus fulfilling the requirements for subgrade construction materials. Currently, this is primarily implemented through three methods: (1) substituting conventional subgrade soil with single-material modified red mud, (2) substituting conventional subgrade soil with composite-material modified red mud, and (3) using red mud-based foamed lightweight soil.

4.1. Single Material Modified BPRM

Single-material modification entails the incorporation of solely one type of modifying agent into BPRM, which can be either traditional cementitious materials like cement or lime, or industrial waste residues (such as steel slag or phosphogypsum. This approach aims to enhance its road performance characteristics.

4.1.1. Modification with Traditional Cementitious Materials

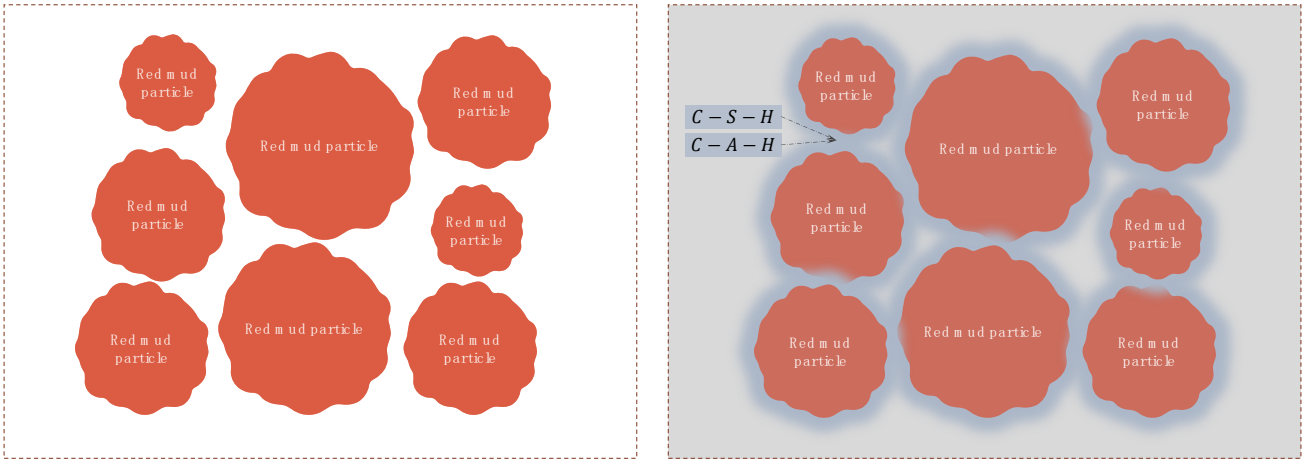
1. Modification Mechanism

As traditional cementitious binders, the incorporation of cement or lime into BPRM markedly improves its mechanical properties through four coupled mechanisms: cement/lime hydration, pozzolanic reactions, carbonation, and ion exchange [49, 81]. The rapid hydration of cement produces a significant amount of calcium silicate hydrate (*C-S-H*), which quickly enhances the early strength of red mud [82]. By contrast, lime cannot self-hydrate into the complex hydration products formed by cement; instead it relies on the reactive silica and alumina inherently present in the red mud to generate cementitious products through pozzolanic

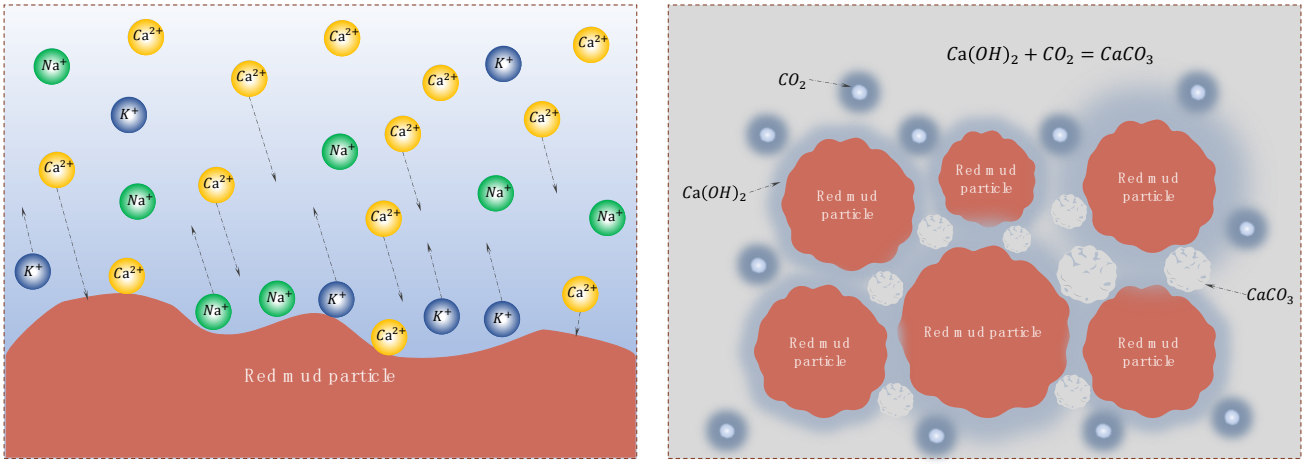
reactions. Strength gain with lime is therefore initially slower, but it progresses to a stable long-term value [49, 83]. Moreover, the carbonation of lime precipitates calcite crystals that infill pores and increase the density of the matrix [81].

Upon mixing cement with BPRM(Fig.9a) , the alkaline environment of the red mud accelerates the hydration reaction of the cement, leading to the formation of $Ca(OH)_2$ and calcium silicate hydrate (*C-S-H*) gel [82]. Concurrently, active silica (SiO_2) and active alumina (Al_2O_3) components within the BPRM react with calcium hydroxide ($Ca(OH)_2$) released during cement hydration through a pozzolanic reaction, generating additional cementitious gels, primarily calcium silicate hydrate (*C-S-H*) and calcium aluminate hydrate (*C-A-H*) [83, 84]. These *C-S-H* and *C-A-H* gels encapsulate and bind the red mud particles, forming a three-dimensional network structure(Fig.9b) [56, 77, 78, 85, 86].

Furthermore, calcium ions (Ca^{2+}) from the cement can undergo ion exchange with lower-valence cations, such as sodium (Na^{+}) and potassium (K^{+}), adsorbed on the surface of the BPRM particles(Fig.9c) [87]. This exchange compresses the thickness of the electrical double layer (EDL), weakens inter-particle repulsive forces and promotes particle agglomeration, thereby reinforcing the three-dimensional network. Additionally, the fine particles of cement hydration products fill the pores within the BPRM microstructure, contributing to a denser coagulated structure [85]. The combined effect of chemical gelation and physical pore filling constitutes a dual synergistic mechanism that markedly strengthens the mechanical performance of BPRM(Fig.9).



(a) (b)



(c) (d)

Fig.9 Mechanism of Single Modification of Red Mud Using Traditional Cementitious Materials (a)red mud particles (b) hydration gelation (c)cation exchange (d)carbonation reaction

The modification mechanism of lime on BPRM shares similarities with that of cement, with the key distinction that lime does not undergo hydration to form multiple complex hydration products like cement. Instead, lime relies primarily on the active SiO_2 and Al_2O_3 components within the red mud. Under alkaline conditions, these components react with lime via pozzolanic reactions to generate *C-S-H* and *C-A-H* gels [83, 87]. Additionally, the $Ca(OH)_2$ from lime gradually reacts with atmospheric CO_2 through carbonation, forming $CaCO_3$ crystals(Fig.9d). These crystals fill pores and enhance structural compactness, thereby improving the strength of the BPRM [81].

Table 3 Mechanisms and key products of BPRM modified by cement and lime

Mechanism	Key Reaction Products	References
Cement hydration	*C-S-H*, *NASH* (sodium aluminosilicate hydrate), hemicarbonate	[88] [82]
Pozzolanic reaction	*C-A-S-H*, zeolitic hydrates	[89] [83]
Carbonation	Calcite, dawsonite	[90] [91]
Ion exchange	Ca^{2+} absorption on RM particles	[87]

The modification mechanisms of cement and lime on BPRM share fundamental similarities but exhibit key differences. Consequently, the technical performance of modified red mud shows both comparable characteristics and distinct variations. When the additive content is $\leqslant$10%, the California Bearing Ratio (CBR) of cement- or lime-modified red mud gradually increases with higher additive dosage, though the rate of improvement progressively diminishes. At lower dosages (<6%), lime-modified red mud demonstrates significantly superior CBR values compared to cement-modified samples at equivalent additive levels. Conversely, at higher dosages (>6%), cement-modified specimens exhibit greater strength (Fig. 10a) [56]. Notably, when lime dosage exceeds 10%, the CBR of lime-modified red mud decreases with further lime addition (Fig. 10b) [86]. Therefore, for both technical and economic reasons, the lime content should be optimised rather than maximised during modification. This non-monotonic behaviour

is corroborated by independent road-base studies: lime-stabilised red mud satisfies strength requirements only within a bounded dosage window, whereas an excess of unreacted lime leaves fines that dilute the matrix and reduce compactness [86]. Quantitatively, red mud stabilised with 3-10 % cement reached 7-day UCS of 0.8-6.0 MPa, whereas 5-30 % lime gave only 0.30-1.67 MPa at 7 days and 0.65-3.60 MPa at 28 days, and its durability criteria were not met - directly confirming the faster, stronger early response of cement relative to the slower pozzolanic development of lime [92].

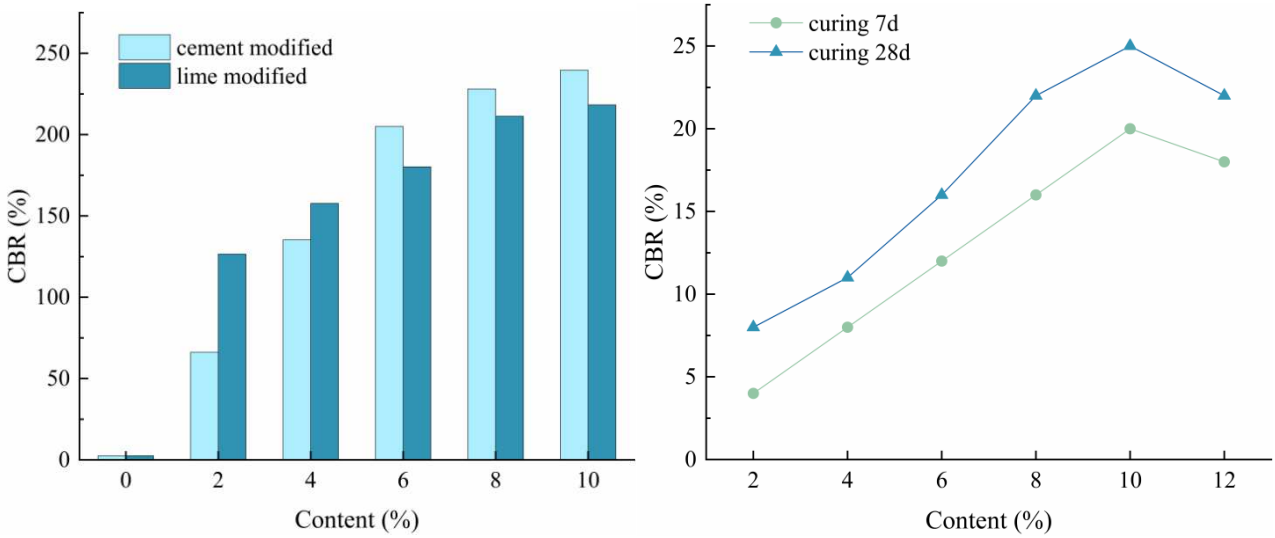


Fig.10 Strength of cement and lime modified BPRM under different dosages [56][86]

Beyond the fundamental reaction mechanisms described above, the choice of a single cementitious binder, Portland cement or lime, represents the two most extensively studied routes for stabilizing BPRM as a road-base or subbase material. Although both binders ultimately exploit the active SiO_2 and Al_2O_3 fractions of the red mud to generate a continuous C-S-H/C-A-H gel network that encapsulates particles and fills pores, their reaction pathways and engineering consequences differ markedly. Cement modification is governed by rapid hydration supplemented by pozzolanic reactions, giving fast early-age strength gain and, above ~6 % dosage, a higher strength than lime at an equivalent binder content [56, 82, 83]. Lime, by contrast, lacks self-hydration into complex hydrates and relies primarily on the slower pozzolanic reaction together with atmospheric carbonation for strength development; its CBR increases with dosage up to ~10 % but declines beyond this optimum because of excess free lime [81, 86]. These distinctions in reaction products, strength evolution, and dosage sensitivity are consolidated in Table 4, which provides a side-by-side comparison to support binder selection for BPRM-based pavement courses.

Table 4. Comparison of cement vs. lime modification of BPRM

Feature	Cement modification	Lime modification	References
Binder hydration	Portland cement hydrates: $C_3S/C_2S+H_2O\rightarrow C-S-H+Ca(OH)_2$	No self-hydration into complex products	[82] [83]
Dominant reactions	Hydration + pozzolanic + ion exchange	Pozzolanic + carbonation	[82] [83] [81]

Cementitious products	C-S-H, C-A-H, residual $Ca(OH)_2$	C-S-H, C-A-H, $CaCO_3$	[82] [83] [81]
Early-age strength	Develops rapidly (fast hydration)	Slower initially (depends on pozzolanic rate)	[49] [82] [92]
Long-term strength	High, continues to gain	Stable once pozzolanic development completes	[49] [86] [92]
Typical UCS	0.8-6.0 MPa (7 d, 3-10% binder)	0.30-1.67 MPa (7 d) / 0.65-3.60 MPa (28 d, 5-30% binder)	[92]
Dosage – CBR trend	CBR rises with dose; above ~6% surpasses lime	CBR rises then declines once lime > 10%	[86] [56]

2. Engineering Applications

The 7-day unconfined compressive strength (UCS) of BPRM modified solely with either cement or lime also demonstrates significant enhancement[56]. At a 10% additive dosage, the maximum 7-day UCS reaches nearly 2.0 MPa(Fig.11). Consequently, BPRM modified with a single cementitious agent (cement or lime) not only satisfies the technical requirements for roadbed fill materials but also meets the strength criteria specified in current Chinese standards for inorganic stabilized subbase layers in Class II and lower-class highways. These criteria refer to the roadbed fill requirements of JTG D30-2015 and to the strength criteria for inorganic binder-stabilised materials in JTG/T F20-2015; because such limits are jurisdiction-specific, they describe Chinese practice only and equivalent criteria elsewhere should be verified separately.

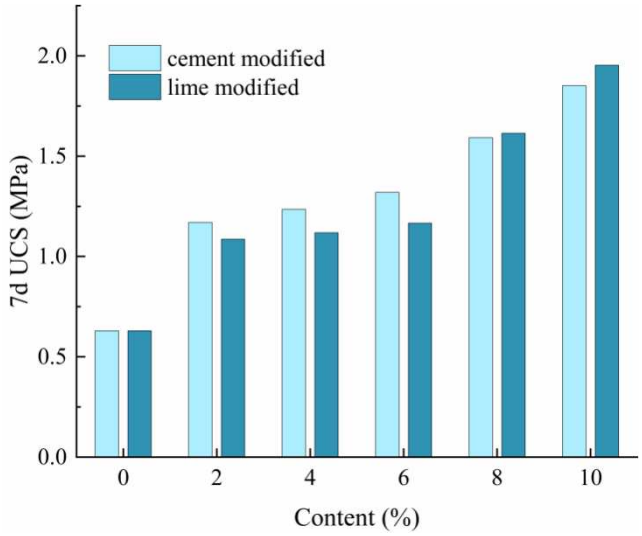


Fig.11 7 d unconfined compressive strength of cement and lime modified BPRM under different dosages[56]

Notwithstanding the satisfactory strength attained by single-binder modification, full-scale engineering practice favors composite stabilization systems. Road subgrade must simultaneously meet comprehensive performance criteria, notably water stability, frost resistance, and long-term durability, that a sole cement or lime addition can hardly secure on its own. Consequently, stabilization of BPRM with a single cementitious agent (cement or lime alone) has, to date, remained largely confined to laboratory strength verification and pilot-scale trials; whereas production-level pavement construction has predominantly adopted blended binders (e.g., cement or lime combined with fly ash, ground granulated blast-furnace slag, or mineral aggregates) to reconcile strength gain with serviceability under field conditions.

4.1.2. Modification with Industrial Waste Residues

1. Modification Mechanism

Industrial waste residues, such as blast furnace slag, steel slag, and desulfurization gypsum, contain appreciable amounts of calcium (*Ca*), silicon (*Si*), aluminum (*Al*), and iron (*Fe*) oxides. These components exhibit latent reactivity and undergo chemical reactions analogous to those of cement and lime. Under alkaline conditions, they participate in hydration and pozzolanic reactions, enhancing the strength of BPRM through cementation and pore-filling effects.

Blast furnace slag (BFS), an industrial by-product of iron smelting, primarily consists of CaO, SiO_2, and Al_2O_3, exhibiting latent reactivity. Modification of red mud with BFS significantly enhances key mechanical properties, including the California Bearing Ratio (CBR), resilient modulus, and unconfined compressive strength (UCS). Notably, these improvements persist under immersed conditions, demonstrating retained strength [93]. Given that reactive components (CaO and SiO_2) constitute approximately 70% of BFS, a composition analogous to ordinary Portland cement, the application parameters established for cement-modified red mud may be referenced for optimal utilization.

Steel slag, a by-product of steel smelting, shares compositional similarities with blast furnace slag but differs primarily in its significant iron oxide (FeO/Fe_2O_3) content. While steel slag significantly enhances mechanical properties such as unconfined compressive strength (UCS) in modified red mud and facilitates rapid strength development, unprocessed steel slag contains notable amounts of free lime (*f-CaO*) and free magnesia (*f-MgO*). These reactive phases induce substantial volumetric expansion in the modified material (Fig. 12) [56]. Furthermore, due to its inherently weak cementitious properties, steel slag-modified red mud exhibits poor strength retention under immersed or freeze-thaw conditions [56]. Consequently, it is recommended to employ aged steel slag treated via thermal steam aging or carbonation curing for red mud modification. Additionally, steel slag-modified red mud should be avoided as roadbed fill in high-precipitation regions or areas subject to freeze-thaw cycles.

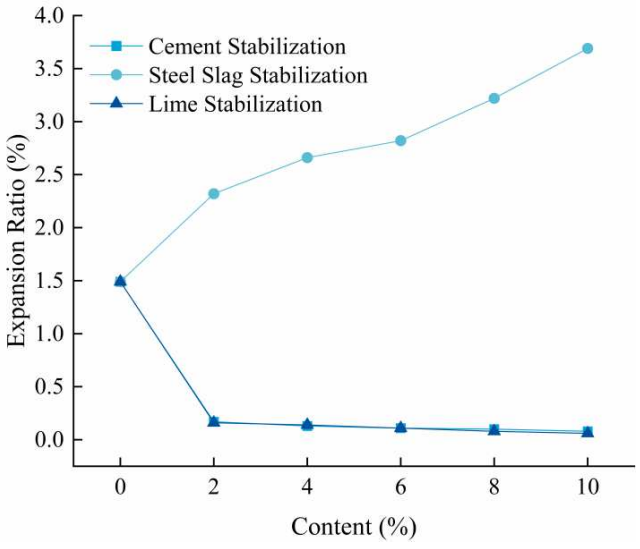


Fig.12 CBR Expansion Rate of Modified Red Mud [56]

Desulfurization gypsum (DG), a by-product of flue gas desulfurization in coal combustion, primarily consists of calcium sulfate dihydrate ($CaSO_4 \cdot 2H_2O$) with minor quantities of Fe_2O_3 and Al_2O_3. Compared to lime or blast furnace slag at equivalent dosages, DG demonstrates relatively weaker enhancement of the California Bearing Ratio (CBR) in modified red mud. Critically, after 24-hour water immersion, DG-modified specimens disintegrate completely [93]. Given this pronounced water sensitivity, similar to steel slag-modified systems, DG-treated red mud is not recommended for roadbed construction in high-precipitation regions or freeze-thaw environments.

2. Engineering Applications

Single-material modification effectively enhances the road performance of BPRM, with significant improvements observed in the California Bearing Ratio (CBR). Laboratory testing confirms compliance with current specifications for roadbed fill materials. However, given the material's persistent strong alkalinity and heavy metal leaching potential, large-scale implementation of single-material modified red mud remains limited in China. According to published literature, Greece pioneered a full-scale test section in the 1990s using red mud modified with 4% (by mass) fly ash. This 75-meter-long test embankment with 3-meter fill height (Fig. 13a) exhibited remarkable performance after five years of service: overall structural integrity was maintained with only 1 cm settlement (Fig. 13b) [94]. This case offers valuable reference for future engineering applications of single-material modified BPRM.



(a) (b)

Fig.13 BPRM embankment in Greece (a)initial period of opening to traffic (b)5 years after opening to traffic [94]

4.2. Composite Modified BPRM

1. Modification Mechanism

Composite modification blends two or more binders, such as cement, lime, steel slag, blast furnace slag, phosphogypsum, or polymers, into a tailored composite modifier at optimized ratios. The modifier is then mixed into BPRM to improve its physico-mechanical properties. The mechanism parallels that of cement or lime stabilization, with the cementitious action of cement and lime as the principal driver. Industrial residues supply reactive oxides (e.g., SiO_2, Al_2O_3, CaO) that form additional cementitious phases. Their synergistic interaction raises the technical performance of BPRM.

Studies confirm that the gain is robust across a wide range of formulations and is anchored in the cementitious action described above. All five investigations report order-of-magnitude increases in California Bearing Ratio (CBR), from 2.6 to 128.5 [56], 4.3 to 124 [40], 6.6 to 389.5 [93], and 2.8 to 94 [95], together with 7-day unconfined compressive strength (UCS) of 1.91 to 5.52 MPa [40, 56, 78, 93, 95]. Critically, Sun Zhaoyun [78] showed that a cement, lime, phosphogypsum, and polymer composite surpassed single-binder treatments at equal dosage, indicating that the improvement arises from component synergy rather than from the dosage of any single constituent. The chemistries involved are diverse, spanning cement, lime, and steel slag with a polymeric chelator [56], cement, lime, phosphogypsum, and polymers [78], cement, phosphogypsum, and polymer [40], lime, blast furnace slag, and desulfurization gypsum [93], and a cement, phosphogypsum, ferrous sulfate, silica, and polyacrylamide system (Heinchem) [95], yet all converge on the same outcome. This convergence is consistent with a mechanism driven by cementitious hydration and polymer adsorption. Benefits extend beyond strength. Shijie Ma et al. [40] lowered the liquid limit from 51.4% to 37.2% (plasticity index 13.3 to 15.1), improving workability, while Wang Chaoyi [93] retained high CBR and a 7-day UCS of 5.52 MPa under immersed conditions, indicating durability.

Table 5. Strength of composition-modified BPRM

Material Composition	Dosage (%)	CBR	7-day UCS (MPa)	References
cement, lime, steel slag, polymeric heavy metal chelator	5	128.5	1.91	[56]
cement, lime, phosphogypsum, polymers	8	/	3.83	[78]
cement, phosphogypsum, polymer	8.7	124	4.5	[40]
Lime, blast furnace slag, desulfurization gypsum	8	389.5	5.52	[93]
cement, phosphogypsum, ferrous sulfate, silica, polyacrylamide	12	94	3.08	[95]

These results consistently indicate that the polymeric/organic fraction improves workability and encapsulates or chelates alkalis and heavy metals, whereas the inorganic fraction supplies hydraulic and pozzolanic reaction products; their synergy raises CBR by one to two orders of magnitude above that of raw BPRM (CBR ≈ 2-7)(Table 5). Beyond the representative formulations above, a broader 2016-2026 literature has systematically examined the component combinations and underlying mechanisms of composite modification, as summarized below.

(1) Sulfate-activated cement-lime-phosphogypsum systems

Building on the cement-lime baseline, adding phosphogypsum opens a sulfate-activated reaction pathway. Shi et al. [96]

optimized a cement-lime-phosphogypsum solidified red mud at a curing-agent mass ratio of cement:lime:phosphogypsum = 8:2:2, obtaining a 7-day UCS of 4.18 MPa, a 28-day splitting tensile strength of 0.256 MPa, and a resilient modulus of 1020 MPa. After five dry-wet and freeze-thaw cycles, the mass change was <2% and the strength-loss index (BDR) exceeded 80%. Mercury intrusion porosimetry (MIP) showed that ettringite (AFt) generated from phosphogypsum fills 0.1-1 μm pores and densifies the matrix, whereas excess AFt drives volumetric expansion and 1-10 μm microcracks that weaken the material. Wang et al. [77] confirmed that, with the total cement plus lime held at 10%, a cement:lime ratio of 8:2 with ~5% phosphogypsum gave a 7-day UCS >3 MPa; SEM revealed needle-like AFt crystals interlocking particles and filling pores, whereas >8-10% phosphogypsum induced expansion damage. These studies show that phosphogypsum acts as a threshold activator: beneficial up to an optimum (~5%) and detrimental beyond it.

(2) Lime-slag-desulfurization gypsum systems

Luo et al. [97] modified BPRM with lime, ground granulated blast-furnace slag (GGBS), and desulfurization gypsum. A double-doped lime-slag blend (10 wt%, 1:1 mass ratio) gave the best performance. It raised CBR to 306.22%, resilient modulus to 123.58 MPa, and UCS to 3.02 MPa. These values represent improvements of +129%, +28%, and +148% over the equivalent single-doped mixes. Leachates of *Cd*, *V*, *Se*, *As*, and fluoride stayed below China's Class I groundwater limits. This supports the use of the stabilized material as an environmentally safe subgrade fill. This finding support the view that GGBS supplies pozzolanic Si-Al, which with lime-derived Ca^{2+} forms additional *C-S-H*/*C-A-S-H* gel.

(3) Red mud-fly ash-desulfurized gypsum geopolymer bases

Several studies replace Portland cement entirely with industrial-waste blends that exploit the intrinsic alkalinity of BPRM as an activator. Qin et al. [98] formulated a red-mud geopolymer subgrade from red mud, fly ash, slag and desulfurized gypsum, evaluating both soaked and unsoaked CBR, permeability, and soaked-strength loss. This study confirm that the alkalinity of BPRM activates *Si-Al* sources (fly ash, slag), yielding binder gels without external cement. This cement-free route meets road-base mechanical requirements and maximizes the co-utilization of bulk solid wastes..

(4) Red mud-coal gangue systems

Liu et al. [99] prepared a Bayer red mud-coal gangue road-base material with fly ash, whose 7-day UCS exceeded 6 MPa. After 20 dry-wet cycles the strength remained 5.98 MPa, and after five freeze-thaw cycles it reached 6.89 MPa, satisfying the relevant Chinese national standards. Crucially, 94.79% of Na^{+} was immobilized at 28 days, an outcome attributed to the *Si-Al* system fixing Na^{+} more effectively. The radioactivity of the raw red mud also met outdoor-building-material limits. This highlights the dual gain of composite systems: strength gain and alkali immobilization.

(5) All-solid-waste binders: red mud-calcium carbide residue-phosphogypsum

A frontier direction eliminates ordinary Portland cement altogether, as shown by Ye et al. [100], who combined red mud,

calcium carbide residue (CCR) and phosphogypsum at 85:10:5 (RM:CCR:PG). This achieved a 7-day UCS of 6.83 MPa, a 412% increase over unreinforced RM (1.33 MPa). CCR supplies Ca^{2+} ions and alkalinity that dissolve the red mud, while PG sulfate further activates the reaction. The hydration products (ettringite, *C-(A)-S-H* and *N-A-S-H*) densify the microstructure and stabilize Na^{+} and heavy metals. Yan et al. [101] advanced an all-solid-waste binder (CGFPA: calcium carbide residue + GGBS + fly ash + phosphogypsum + graphene additive) for red-mud subgrade. Its hydration products (*C-S-H*, *C-A-S-H*, monosulfate AFm, hydrotalcite) solidify and stabilize the red mud through adsorption and cementation, meeting strength and toxicity-leaching specifications.

6. Nano-SiO2 synergistic modification

At the micro-level, Chen et al. [102] showed that nano-SiO_2 synergizes with gypsum and cement in red-mud stabilized soil. The optimal NS1CS6PC3 mix (1% nano-SiO_2, 6% gypsum, 3% cement) reached a 7-day UCS of 2.748 MPa, greater than the sum of the individual effects ("1 + 1 > 2"). Nano-SiO_2 accelerates *C-S-H* formation and refines pores, illustrating how nanoscale additives can further upgrade composite binders.

Table 6. Key findings of composite system

Composite system	Main binders / optimal ratio	Key finding / modulus
Cement-lime-phosphogypsum	cement:lime:PG = 8:2:2	7-day UCS = 4.18 MPa: Mr = 1020 MPa; BDR > 80% after 5 dry-wet/FT [96]
Cement:lime + phosphogypsum	cement:lime = 8:2, ~5% PG	7-day UCS > 3 MPa; Needle-like AFt fills pores [77]
Lime + slag + desulf. gypsum	10% total lime+slag, 1:1	7-day UCS = 3.02 MPa; CBR = 306.22%, Mr = 123.58 MPa [97]
Red mud + fly ash + desulf. gypsum	cement-free geopolymer	Alkali of RM activates *Si-Al* [103]
Red mud - coal gangue (+FA)	road-base blend	7-day UCS > 6 MPa; *Na*+ fixed 94.79%; radioactivity OK [99]
Red mud - CCR - phosphogypsum	RM:CCR:PG = 85:10:5	7-day UCS = 6.83 MPa; +412% vs RM; all-solid-waste [100]
All-solid-waste CGFPA	CCR + GGBS + FA + PG + graphene	*C-S-H*/AFm/hydrotalcite; toxicity OK [101]
Nano-SiO2 + gypsum + cement	NS1CS6PC3 (1% NS, 6% G, 3% C)	7-day UCS = 2.75 MPa; Synergy '1+1>2'; refines pores [102]
Modified RM subgrade (field)	composite binder	Mr > 90 MPa; dynamic def. <=140 MPa; FWD <100 [40]

Viewed together, the six families above - though formulated from very different waste streams - converge on a small set of coupled mechanisms. Collectively, composite modification of BPRM exploits five complementary actions: (i) sulfate activation by phosphogypsum/desulfurization gypsum generating AFt that fills sub-micron pores and boosts early strength, provided the dosage is kept below the expansion threshold; (ii) supplementary calcium from lime, quicklime or calcium carbide residue that drives pozzolanic and carbonation reactions; (iii) pozzolanic Si-Al from fly ash, slag or coal gangue forming *C-S-H*/*C-A-S-H* gels and, importantly, fixing exchangeable Na^{+}; (iv) polymer/organic components that improve workability, bridge particles and chelate heavy metals; and (v) alkali self-activation of BPRM, which can substitute for external cement in geopolymer routes. Durability under dry-wet and freeze-thaw cycling is generally satisfactory when the mix is optimized (BDR > 80%), and Na+/heavy-metal

immobilization commonly meets environmental standards, enabling large-scale trials-e.g., the modified BPRM subgrade assessed at field scale with resilient modulus > 90 MPa, dynamic deformation modulus up to 140 MPa and FWD < 100 (0.01 mm) [40].

2. Engineering Applications

Compared to single-binder modification, composite-modified BPRM exhibits substantially enhanced 7-day unconfined compressive strength (UCS), typically exceeding 3 MPa (Table 5 and 6). This performance satisfies strength requirements for roadbed fills and inorganic stabilized subbase layers across all highway classes, and also meets specifications for base layers in Class II and lower-category highways. Building on this foundation, Shandong Province enacted the local standard Technical Specifications for Application of Red Mud (Bayer Process) in Highway Subgrades (DB37/T 3559-2019) in 2019. This regulation defines critical parameters, including dosage ranges for red mud modifiers, technical performance criteria for modified red mud, cross-sectional design of clay-wrapped modified red mud embankments, and compaction standards, thereby providing a normative framework for large-scale implementation. Composite-modified BPRM has now been deployed in highway and municipal road projects across Shandong and other regions. Key demonstrations include: These strength requirements are those specified for subgrade fills and inorganic binder-stabilised subbase layers in JTG D30-2015 and JTG/T F20-2015 respectively, and for base courses of Class II and lower-grade highways under Chinese practice; other jurisdictions adopt different limits and are not covered by this comparison.

Highway Application:

During the Jinan-Qingdao Expressway expansion project, a 4,900-m test section used composite-modified red mud to replace the originally designed lime-stabilized soil in its upper 20 cm subgrade layer (Fig. 14a) [40]. Field measurements confirmed that all subgrade-surface deflections fell below 100 (0.01 mm).

Municipal Road Application:

In the Binzhou Beihai Recycling Park Phase I road project, a 100 m test section employed composite-modified red mud instead of lime-fly ash stabilized soil in the upper 40 cm subgrade (Fig. 14b) [78]. Field tests recorded deflections between 47.2–138.9 (0.01 mm), while plate loading tests demonstrated a subgrade resilience modulus $\geqslant$70 MPa.

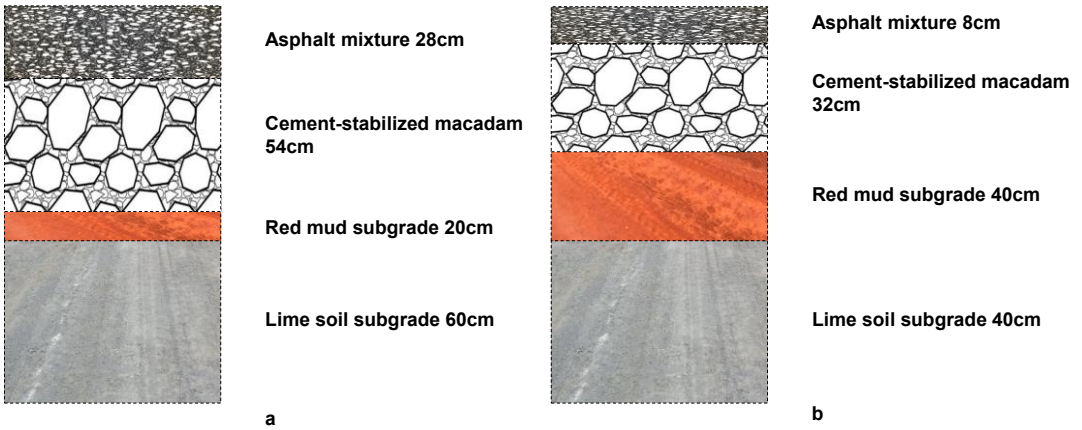
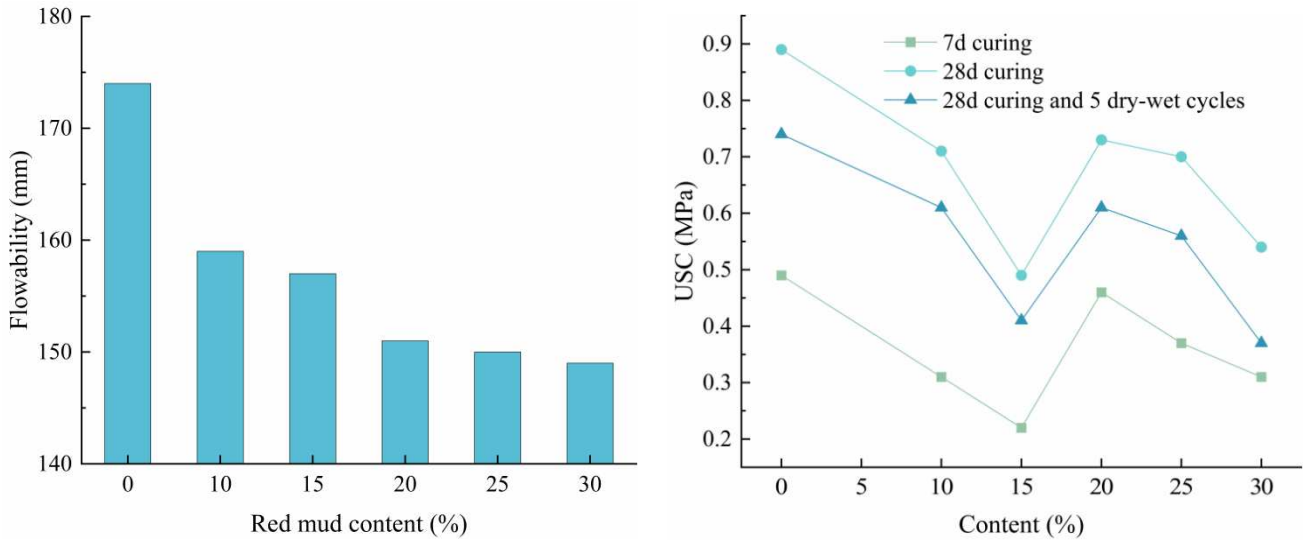


Fig.14 Pavement structure of the demonstration section (a) Jinliqing Expressway (b) Binzhou Beihai venous industrial park [40, 78]

4.3. BPRM Based Foamed Lightweight Soil (BPRM-FLS))

Foamed lightweight soil (FLS), a novel lightweight fill material formed by introducing foaming agents into a cementitious paste, contains abundant closed air voids and exhibits moderate strength. Characterized by its porous structure, low density, and construction efficiency, FLS is primarily deployed in special highway sections prone to differential settlement. Typical applications include road-widening zones during expressway upgrades, high-fill embankments, and road-bridge transition sections. Conventional cement-dominated FLS faces significant limitations: high cement consumption, pronounced cracking tendency, and substantial energy footprint. To address these technical and ecological challenges, recent advances leverage BPRM as a sustainable raw material. By harnessing synergistic modification effects between red mud and cement, RM-FLS achieves partial cement replacement while enhancing performance metrics, demonstrating considerable progress in research and application.

Ou et al. [104] modified cement foamed lightweight soil (FCLS) into a cement-red mud composite cementitious material foamed lightweight soil (FMLSR) by partially replacing cement with BPRM at 10%-30%. As the red mud replacement ratio increased, the flowability of FMLSR rapidly decreased and gradually stabilized (Fig. 15a). Meanwhile, the unconfined compressive strength (UCS) first decreased, then increased, and finally declined (Fig. 15b). At a 20% BPRM replacement ratio, the 28-day UCS of FMLSR reached a maximum of 0.73 MPa. This satisfies the Specifications for Design of Highway Subgrades (JTG D30-2015) for subgrade fill in highways, first-class roads (subgrade and subbase), and second-class or lower roads (subgrade and subbase alike). This demonstrates the feasibility of engineering applications for FMLSR.



(a) (b)

Fig.15 Influence of red mud content on properties of foam lightweight soil (a) flowability (b) unconfined compressive strength [104]

The partial replacement of cement by BPRM inevitably reduces FLS fluidity, while crack resistance remains a concern for field placement. Two recent studies have addressed these weaknesses at the material level. To recover the fluidity lost when cement is replaced by red mud, Chuanyi et al. [105] examined how the water-binder ratio and water-reducing admixtures affect red-mud-based FLS. In a system of BPRM and ground granulated blast-furnace slag (GGBS), both a polycarboxylate and a naphthalene-based high-efficiency water reducer improved slurry fluidity. The naphthalene-based admixture gave the larger fluidity gain and also raised compressive strength, whereas the polycarboxylate admixture improved fluidity but lowered compressive strength. To further enhance strength and crack resistance, Li et al. [106] added polyester (PP), polypropylene (PES), and kenaf (KF) fibers to a composite cementitious FLS made from red mud, cement, lime, and fly ash, and evaluated fiber type, length, and dosage. All three fibers markedly raised the unconfined compressive strength. At a fiber length of 12 mm and a dosage of 0.75%, the strength peaked at 0.875 MPa (PP), 0.81 MPa (PES), and 0.68 MPa (KF). These values represent increases of 145.8%, 135.8%, and 113.3% over the untreated specimen, respectively.

Building on these material advances, Lin [107] applied a BPRM-based cementitious material (BPRM, GGBS, cement, and quicklime) in the Shandong Zhanhua-Linyi Highway Construction Project. Treating strength and fluidity as the governing design criteria, he specified distinct water-binder ratios and strength targets for two pavement layers. For the embankment layer, the designed wet density was 800 kg/m³ at a water-binder ratio of 0.70, with 7-day and 28-day UCS of 0.69 MPa and 0.93 MPa, respectively. For the subgrade-bed layer, the wet density was 1,000 kg/m³ (same water-binder ratio of 0.70), with 7-day and 28-day UCS of 0.91 MPa and 1.29 MPa. Following this design, red-mud-based FLS subgrades of 68 m and 160.5 m were placed at two bridge-approach transition sections, consuming 23,029.5 tonnes of BPRM. Relative to cement-based FLS, the approach saved

RMB 4.6207 million in material costs, a roughly 20% reduction in comprehensive cost.

5. Waste-for-Soil Stabilization: BPRM as Cementitious Additive for Subgrade Soil Improvement

The strong alkalinity of BPRM supplies an alkaline environment that drives reactions within cementitious systems. This enables synergistic interactions with cement and other solid wastes to form novel cementitious binders, applicable to the improvement of special soils (soft clay, silt, loess) and the stabilization of conventional subgrade soils.

High-plasticity soft clay tends to lose strength through moisture-induced swelling. Wan et al. [57] developed a composite cementitious binder by combining red mud (RM), phosphogypsum (PG), and cement. The mix contained 8% cement and 10% combined RM-PG, tested at RM/PG mass ratios of 10/0, 7.5/2.5, 5/5, 2.5/7.5, and 0/10 to probe their synergy. UCS tests on the modified clays (Fig. 16) showed that adding RM-PG to cement markedly raised the 7-day strength, an effect attributed to the alkaline environment supplied by RM that accelerated cement hydration. As the RM/PG ratio fell from 10/0 to 7.5/2.5, the acidic PG lowered the system pH but contributed extra Ca^{2+} and SO_4^{2-} ions that promoted ettringite (AFt) formation [108]. The resulting AFt crystals filled interparticle voids in the modified clay matrix, raising strength. A further drop in the RM/PG ratio produced two adverse effects: (i) weaker alkalinity that reduced the activation effect, and (ii) excessive AFt expansion driven by the higher PG content. These effects caused microcracking and structural degradation in the cementitious system [109], thereby lowering the clay strength. S. Wang et al. [44] extended this approach to silty soils with RM-PG-cement blends and observed analogous trends. Their results recommended an optimal RM/PG ratio of 7:1 to keep the cementitious system within a neutral-to-weakly alkaline range.

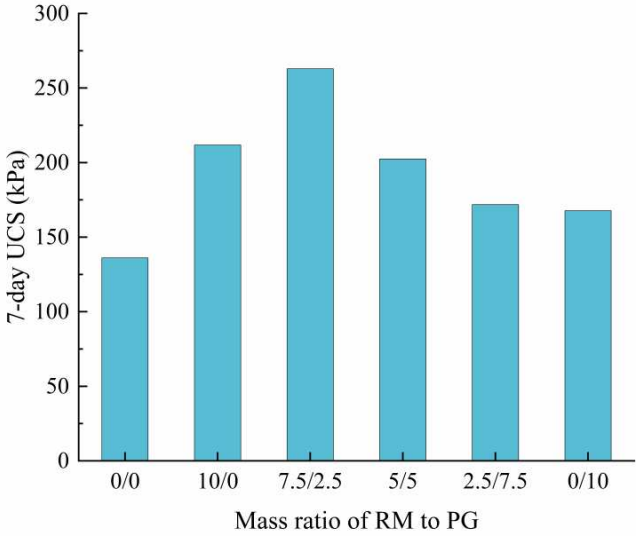


Fig.16 Strength variations with different mass ratio of RM to PG [57]

For typical collapsible loess, R. Chen et al. [110] stabilized the soil with 5% cement and 5%-30% red mud (RM). The unconfined compressive strength (UCS) first rose and then fell as the RM dosage increased. Peak strength occurred at 15%-20% RM, reaching 2.4 MPa after 7 days (Fig. 17).

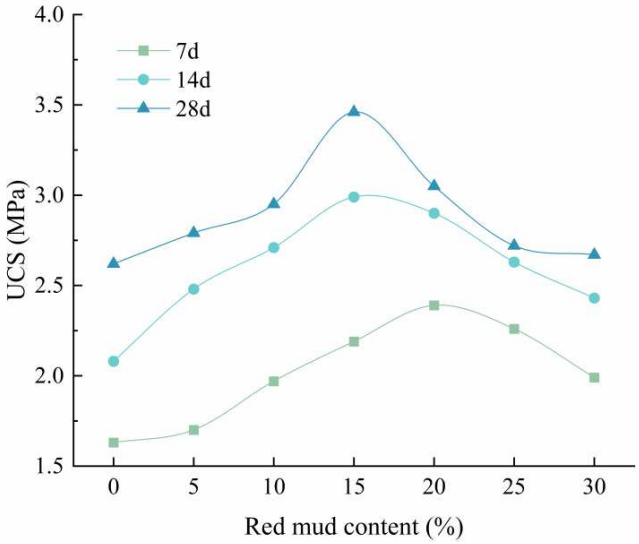


Fig.17 Unconfined compressive strength of red mud stabilized soil [110]

SEM examination showed that moderate RM addition strengthened the stabilized matrix through two mechanisms. First, cement hydration products coated the loess particles (Figs. 18a, b) and progressively bound the dispersed grains into an integrated mass. Second, the added RM particles filled the interparticle voids (Fig. 18c), densifying the structure and raising compressive strength. Beyond the optimum RM content, the effect reversed. Excess RM adhered to the hydration-coated aggregates (Fig. 18d), weakened the cementation between loess particles, and disrupted the stabilized cementitious system, thereby lowering compressive strength.

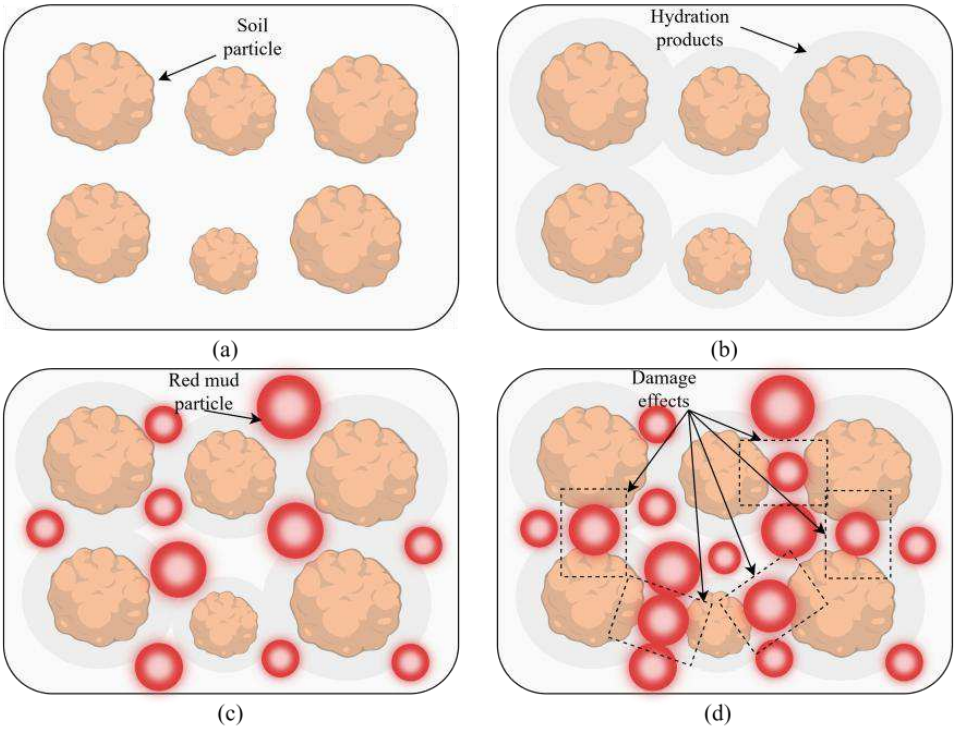


Fig.18 Mechanism of red mud-cement composite stabilized soil

Poorly graded silty soils from the Yellow River alluvial plain show strong capillarity, liquefaction susceptibility under dynamic loads, and poor compactability. To address these weaknesses, Li Xia et al. [111] introduced flexible asphalt into an RM-based cementitious system. The RM acts as a carrier that changes the ambient-temperature dispersion of asphalt and raises its specific surface area. In RM's strongly alkaline medium, asphalt adheres more firmly to soil particles. During high-temperature softening, the dispersed asphalt fines progressively fill the interparticle voids, raising the strength of the composite stabilized soil. The resulting material, termed the RM-flexible consolidator (RFC), exhibits semi-flexible behaviour. Relative to conventional RM-based cementitious materials, it raises soil strength and also allows autogenous healing of micro-damage within the stabilized matrix.

Laboratory tests and field applications confirm that RM-based cementitious materials meet the technical requirements for subgrade fillers. They also satisfy the design criteria for base and subbase courses under light to medium traffic on Class II and lower highways. Guided by the optimum mix from laboratory tests, a 200 m trial section was built with RFC-stabilized silt on a rural highway in Qihe County, Shandong Province. The treatment added 7% RFC and 3% cement to alluvial-plain silty soil [111]. Field measurements showed that the stabilized silt reached a 7-day UCS of 0.86 MPa and a CBR of 75.3%. Mean deflection (0.01 mm) measured 44.3 in the stabilized layer and 25.5 at the pavement surface. The requirements referred to here are those of JTG D30-2015 for subgrade fills and of JTG/T F20-2015 for base and subbase courses under light to medium traffic in China; the grading of highways and the corresponding strength limits are not identical outside China.

6. Stiffness and deformation behaviour under traffic loading

Strength indicators such as CBR and UCS describe bearing capacity at a single loading event, but pavement design also requires stiffness and deformation parameters that control rutting and the accumulation of permanent deformation over the service life [80, 119]. Evidence on these parameters for BPRM-based materials is still scattered, and the mechanics-oriented treatments available so far have quoted strength almost exclusively.

Resilient modulus has been reported for binder-modified red mud. Luo et al. [97] raised the resilient modulus of a lime, ground granulated blast-furnace slag and desulfurization gypsum blend to 123.58 MPa together with a CBR of 306.22%, showing that composite modification improves elastic stiffness and not only compressive strength. Field evidence points in the same direction: the 100 m demonstration section at Binzhou Beihai Recycling Park recorded deflections of 47.2-138.9 (0.01 mm) in service [78].

Under repeated traffic loading the response cannot be inferred from static strength tests. Liu et al. [80] characterised the dynamic characteristics of cement-modified red-mud-based silty soil under traffic load by hollow cylinder torsional shear testing, and Chen et al. [119] examined the dynamic properties and the environmental impact of waste red-mud-treated loess under adverse

conditions. Long-term cyclic response has also been addressed: Liu et al. [123] evaluated the deformation properties of red-mud-reinforced volcanic ash under long-term cyclic loading, and Xu et al. [122] performed large-scale cyclic triaxial tests on improved coarse-grained red mudstone soil, applying cyclic stress from 25 to 225 kPa in 25 kPa increments at a frequency of 2 Hz with 1,000 or 2,000 cycles per stage. Near optimum moisture content the cumulative strain at failure was about 1% after 14,000-16,000 cycles, while at moisture content 2% wet of optimum the strain exceeded 10% after only 3,000-4,000 cycles; cumulative strain decreased as the confining pressure rose from 20 to 50 kPa. Dixit et al. [25] additionally characterised red mud blended with bottom ash as a subgrade geomaterial, extending the evidence base beyond strength alone.

Taken together, these studies indicate that BPRM-based materials gain stiffness under confinement but lose it as the moisture condition departs from optimum, and that permanent deformation rather than compressive strength is what limits their service performance. Because several road administrations now derive design parameters from cyclic triaxial testing instead of CBR, the shortage of such data for red-mud materials is, in the present review, a more practical barrier than insufficient strength.

7. Environmental Safety Assessment of BPRM in Subgrade Engineering

The inherent strong alkalinity and presence of hazardous heavy metals (*Cr*, *Cd*, *Pb*, etc.) in BPRM may pose environmental risks including corrosivity, leaching toxicity, and potential soil/groundwater contamination during subgrade applications. Rigorous environmental risk assessment is therefore essential prior to implementation.

7.1. Corrosion Risk Assessment

BPRM is strongly alkaline. Its pore-water pH typically falls between 10 and 12 in Chinese sources and reaches 13.5 in international studies [4, 112, 113]. When placed in subgrade, it reacts with supplementary cementitious materials (cement, lime, fly ash, phosphogypsum) through hydration, cation exchange, and carbonation. These reactions lower pH by two routes: chemical neutralization of free alkali and conversion of alkalinity-bearing phases into stable solids. In RM-phosphogypsum-stabilized loess, pH falls progressively below 11 as the phosphogypsum dosage rises and eventually settles in the alkaline-neutral transition range [57, 114]. Gypsum and carbonation are established alkalinity-control routes. Gypsum amendation reduces residue alkalinity and salinity [115], and CO_2 mineral carbonation can drive a red mud slurry from pH ~10 to near neutral [116]. The high pH also governs environmental mobility. In alkaline leachates, oxyanionic trace metals such as *As*, *Cr*, *Mo*, *Se*, and V become markedly more mobile [117]. pH reduction therefore curbs both corrosivity and metal-leaching risk. Engineered red mud – fly ash – gypsum blends have been assessed for both strength and leaching as geomaterials [118]. Proper mix design lets modified BPRM meet acceptance criteria for subgrade and base applications.

Under Chinese regulation, the corrosivity identification standard GB 5085.1-2007 classifies an industrial solid waste as hazardous when its leachate pH is ⩾12.5 or ⩽2.0. This threshold mirrors the international corrosivity characteristic (pH ⩽2.0 or ⩾12.5). The general industrial solid waste standard GB 18599-2020 designates wastes with leachate pH outside 6-9 as Class II. On this basis, neither raw BPRM nor its modified products used in road base in China are currently classified as hazardous waste; both are assigned Class II general industrial solid waste. Where interim stockpiling is required, Class II storage rules mandate anti-seepage liners and leak-monitoring systems.

7.2. Heavy Metal Leaching Toxicity Risk

The BPRM used in subgrade engineering, along with other industrial solid waste materials modified synergistically, contains harmful substances such as mercury (*Hg*), lead (*Pb*), cadmium (*Cd*), nickel (*Ni*), arsenic (*As*), hexavalent chromium (Cr^{6+}), and fluoride (F^-). These contaminants can be leached and infiltrate into the soil and groundwater (Fig. 19) through dissolution, scouring, diffusion, and other pathways under the action of rainfall and internal seepage within the pavement structure, thereby posing risks to the surrounding environmental safety.

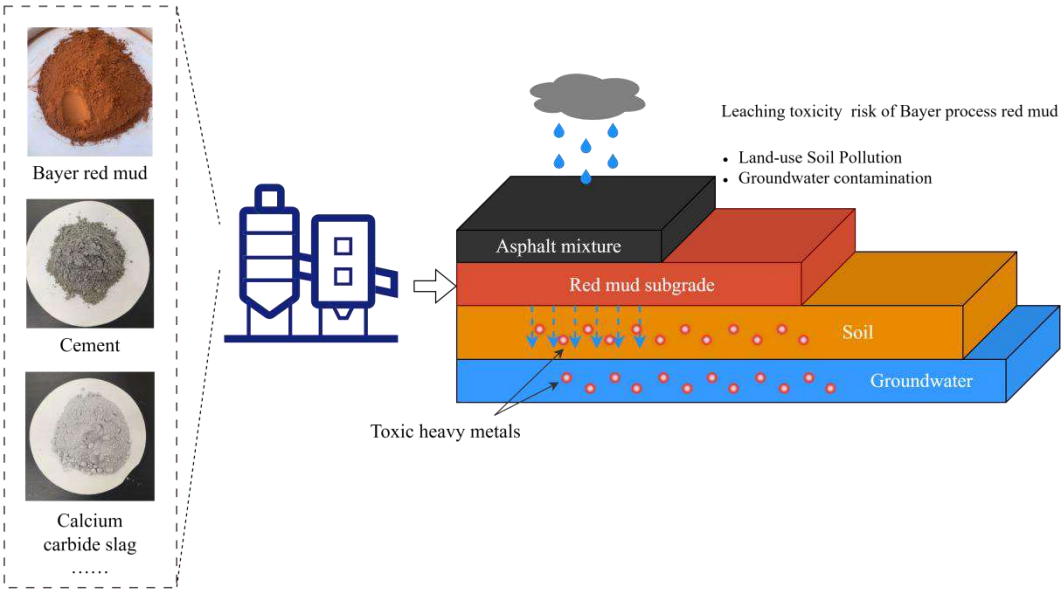


Fig.19 Schematic diagram of leaching toxicity and groundwater pollution risk of BPRM subgrade

7.2.1. Leaching Toxicity Identification

Most studies quantify harmful constituents in BPRM using the element-determination protocol of the Chinese standard GB 5085.3-2007 (Identification Standards for Hazardous Waste: Leaching Toxicity Identification). This protocol is applied to both raw BPRM and composite-modified BPRM used as subgrade material. Typical characteristic pollutants were selected for analysis, including manganese (*Mn*), cadmium (*Cd*), nickel (*Ni*), lead (*Pb*), vanadium (*V*), selenium (*Se*), antimony (*Sb*), arsenic (*As*),

hexavalent chromium (Cr^{6+}), and fluoride (F^-). Their concentrations in raw and modified BPRM subgrade materials are compiled in the table below:

Table 7. Leaching toxicity test results of BPRM

Test parameter	Group 1		Group 2		Group 3		Leaching toxicity standard limits	Groundwater quality class III standard limits
	Rawl red mud	Modified red mud	Rawl red mud	Modified red mud	Rawl red mud	Modified red mud		
Mn	＜0.003 6	＜0.003 6	＜0.01	＜0.01	/	/	/	≤0.1
Cd	0.001 6	0.001 4	＜0.004	＜0.004	0.000 2	0.000 6	≤1	≤0.005
Ni	＜0.001 8	＜0.001 8	＜0.02	＜0.02	0.000 3	0.004 8	≤5	≤0.02
Pb	＜0.004 2	＜0.004 2	＜0.02	＜0.02	0.001 8	0.002 5	≤5	≤0.01
V	0.748	0.061 7	0.28	0.28	/	/	/	/
Se	0.117	0.059 1	0.001 1	0.001 1	/	/	≤1	≤0.01
Sb	＜0.003 2	＜0.003 2	＜0.02	＜0.02	/	/	/	≤0.005
As	0.229	0.036	0.002 7	0.002 7	0.023	0.930 0	≤5	≤0.01
Cr^{6+}	＜0.004	＜0.004	0.031	0.009	0.013	0.006 4	≤5	≤0.05
F^-	0.137	0.002 82	2.56	2.43	/	/	≤5	≤1.0
References	[93]		[78]		[119]			

Leaching toxicity tests against GB 5085.3-2007 (Identification Standards for Hazardous Waste: Leaching Toxicity Identification) indicate that both raw BPRM and modified BPRM used in subgrade satisfy the regulatory limits. Neither is classified as hazardous waste. Against the Class III limits of the Groundwater Quality Standard GB/T 14848-2017 (centralized drinking-water sources and industrial/agricultural use), however, the leachate may still approach or exceed the benchmark for several ions. Elevated concentrations can appear for selenium (*Se*), arsenic (*As*), hexavalent chromium (Cr^{6+}), and fluoride (F^-). Such potential exceedances warrant close monitoring when BPRM-based materials are deployed in the field.

7.2.2. Leaching Toxicity Risk under Practical Conditions

Standardized test methods quantify hazardous-substance concentrations in modified BPRM subgrade materials, yet they capture only part of the picture. They do not fully represent seepage and leaching under real subgrade conditions. In recent years, studies have therefore combined laboratory tests, computational simulation, and field monitoring to track seepage-driven leaching in realistic settings.

For laboratory simulation, several studies adopted the EU EA NEN 7375 leaching test [5, 95]. They paired it with site-relevant scenarios such as rainfall and groundwater. Targeted extractants were refreshed at fixed intervals (0.25, 1, 2.25, 4, 9, 16, 36, and 64 days) to measure released hazardous substances. Although EA NEN 7375 reproduces long-term leaching trends, its extractant stays nearly static between replacements and thus poorly mimics groundwater seepage.

Wang [93] addressed this gap by building a dynamic leaching test with continuous water flow (Fig. 20), derived from the

semi-dynamic EA NEN 7375 protocol. The hydraulic setup reproduced groundwater seepage at a flow rate of 0.3 m/h with stable water levels. Leachate was sampled at 1, 3, 7, 14, 28, 64, and 90 days to track hazardous-substance concentrations.

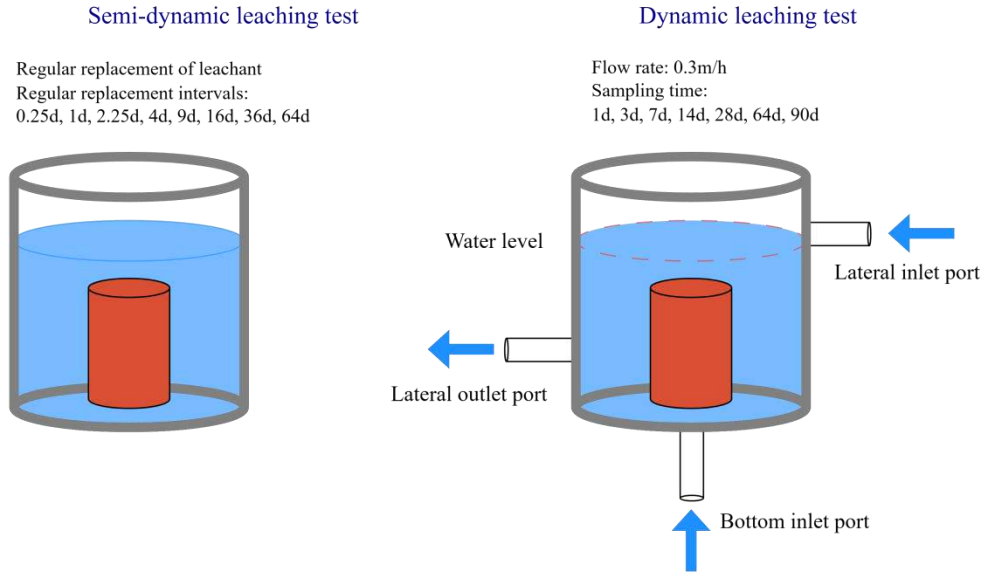


Fig.20 Schematic diagram of leaching test of BPRM subgrade [93]

Coupling mathematical simulation with laboratory data, researchers built models to analyze how hazardous substances are released from modified BPRM subgrade materials. Specifically, the leaching, scouring, and diffusion of contaminants were characterized from the log-slope of cumulative release against time within each semi-dynamic leaching cycle [5, 93]. In general, contaminants leave these materials mainly through precipitation-driven leaching and groundwater seepage. Over long leaching periods, dilution drives the release rates of various hazardous substances toward stabilization.

Beyond laboratory and simulation work, some studies have adopted field monitoring. For example, groundwater monitoring wells were installed in BPRM subgrade test sections [78]. Water samples were taken at 14, 28, 42, 56, 90, 120, 150, and 180 days after construction to measure hazardous-substance concentrations. Although individual pollutants followed different trajectories, their overall trends matched the simulations. Concentrations generally fell and then stabilized, so the risk to human health remains controllable.

8. Conclusion and Prospects

Relative to earlier reviews of red mud in road engineering [9, 45, 48, 49], the distinctive contribution of this review lies in treating waste-based soil replacement and waste-based soil stabilisation as two separate design logics, in consolidating the coupled mechanisms of composite modification into one framework, and in carrying the environmental evidence from static batch leaching through dynamic column tests to coupled modelling and field monitoring.

Through “waste-based soil replacement” and “waste-based soil modification”, BPRM has proved feasible across multiple subgrade scenarios. These include modified red-mud subgrade, red-mud-based foamed lightweight soil, and red-mud-improved stabilized soil. Some findings have already reached large-scale engineering application. Moreover, the environmental risks of using BPRM in subgrade works are controllable. This opens a new route for the reduction and comprehensive utilization of BPRM.

To advance the large-scale reduction of BPRM, future work must deepen research across several key areas. This spans traditional disciplines such as materials science and civil engineering, and demands stronger cross-disciplinary links with environmental science, chemical engineering, and related fields.

(1) Dehydration and pretreatment of BPRM

Wet-process BPRM has a high water content. Laboratory studies can adopt heat drying, but full-scale projects require large drying equipment, raising costs and limiting use. Two aspects deserve attention:

Emission process optimization. Further work on filtration, mechanical dewatering, and related equipment should shift BPRM from “wet discharge” to “dry discharge”, removing the root cause of excess moisture.

Composite dehydration schemes. Given continued wet discharge, low-cost strategies that combine mechanical methods with high-performance water-absorbing materials should be developed for economically viable dewatering.

(2) Universal design methods for multi-solid-waste synergy with BPRM

Current studies show that BPRM-based materials gain markedly better performance through synergy with various solid wastes. Yet, because different wastes differ greatly in composition and pH, composite preparation still relies on empirical trial-and-error, inflating the experimental workload. To move beyond this, future work should analyze the strength-formation mechanisms of BPRM composites: hydration, pozzolanic reactions, and ion exchange. By rating how chemical components of BPRM and other wastes contribute within synergistic cementing systems, researchers can prioritize the key reactive species. Drawing on quantitative indices from cement-clinker design, the silica modulus (SM), alumina modulus (IM), and lime saturation factor (LSF) should guide a quantifiable, tunable, and standardized compositional design method.

(3) Long-term heavy-metal leaching characteristics of BPRM subgrade materials

BPRM carries hazardous species such as mercury (Hg), lead (Pb), cadmium (Cd), nickel (Ni), arsenic (As), hexavalent chromium (Cr^{6+}), and fluorides. In red-mud subgrades, these contaminants can reach groundwater through leachate pathways. Two aspects require attention:

Long-term field monitoring. Full-scale BPRM subgrade projects should embed observation points to track contaminant dispersion in the field. Coupling in situ measurements with laboratory simulations can reveal how rainwater and groundwater seep through the materials. Key variables, including seepage volume, duration, and distance and their effects on contaminant concentration, need systematic study to build predictive dispersion models.

Barrier method development. Guided by the seepage and dispersion mechanisms of hazardous substances, targeted work on isolation layers, filtration layers, and other interception techniques should reduce environmental risk.

(4) Life-cycle assessment and carbon footprint

Beyond mechanical and environmental compliance, the bulk utilization of BPRM in subgrade works should be evaluated by life-cycle assessment (LCA) to quantify energy consumption, carbon emissions, and ecotoxicological impacts relative to conventional fills. Recent LCA studies on red-mud-based geopolymer paving blocks and one-part alkali-activated red-mud – fly-ash subgrade materials confirm substantial global-warming-potential reductions compared with ordinary Portland cement, while identifying alkali activators and electricity as the main contributors [120, 121]. Integrating LCA with the field-monitoring and barrier strategies above would support low-carbon, standards-compliant BPRM subgrade deployment at scale.

References

1. Kannan P, Banat F, Hasan SW, Abu Haija M (2021) Neutralization of Bayer bauxite residue (red mud) by various brines: A review of chemistry and engineering processes. Hydrometallurgy 206:105758. https://doi.org/10.1016/j.hydromet.2021.105758
2. Khairul MA, Zanganeh J, Moghtaderi B (2019) The composition, recycling and utilisation of bayer red mud. Resour Conserv Recycl 141:483–498. https://doi.org/10.1016/j.resconrec.2018.11.006
3. Liu D-Y, Wu C-S (2012) Stockpiling and comprehensive utilization of red mud research progress. Materials 5:1232–1246. https://doi.org/10.3390/ma5071232
4. Reddy PS, Reddy NG, Serjun VZ, et al (2020) Properties and assessment of applications of red mud (bauxite residue): Current status and research needs. Waste Biomass Valorization 12:1185–1217. https://doi.org/10.1007/s12649-020-01089-z
5. Ji W, Liu L, Tan Q, Li J (2025) Red mud used as roadbed material: Revealing the long-term leaching characteristics of heavy metals and associated health risk. J Environ Chem Eng 13:115166. https://doi.org/10.1016/j.jece.2024.115166
6. Zhao Y, Qiang S (2025) Exploring the potential of bayer red mud: Toward self-sensing cementitious composites. Construction and Building Materials 460:139850. https://doi.org/10.1016/j.conbuildmat.2024.139850
7. Zhang R, Zheng S, Ma S, Zhang Y (2011) Recovery of alumina and alkali in bayer red mud by the formation of andradite-grossular hydrogarnet in hydrothermal process. J Hazard Mater 189:827–835. https://doi.org/10.1016/j.jhazmat.2011.03.004
8. Gomes HI, Mayes WM, Rogerson M, et al (2016) Alkaline residues and the environment: a review of impacts, management practices and opportunities. Journal of Cleaner Production 112:3571–3582. https://doi.org/10.1016/j.jclepro.2015.09.111
9. Jia K, Zhou Z, Singh SV, Wang C (2024) A review of the engineered treatment of red mud: Construction materials, metal recovery, and soilization revegetation. Results Eng 24:102927. https://doi.org/10.1016/j.rineng.2024.102927

10. Liu W, Chen X, Li W, et al (2014) Environmental assessment, management and utilization of red mud in China. Journal of Cleaner Production 84:606–610. https://doi.org/10.1016/j.jclepro.2014.06.080
11. Soğancı AS, Yenginar Y, Özkan İ, et al (2024) Waste management of red mud and fly ash to utilize in road subgrade material. Sustainability 16:2987–2987. https://doi.org/10.3390/su16072987
12. Tan Q, Yang Q, Ye C, et al (2024) Utilization of red mud in high-performance grouting material for semi-flexible pavement. J Cleaner Prod 454:142240. https://doi.org/10.1016/j.jclepro.2024.142240
13. Aslam MMA, Sun T, Dai M, et al (2024) Technologies for recovery of iron from red mud: Processes, challenges and opportunities. Sustainable MaterTechnol 41:e01053. https://doi.org/10.1016/j.susmat.2024.e01053
14. Li G, Liu J, Yi L, et al (2024) Bauxite residue (red mud) treatment: Current situation and promising solution. Sci Total Environ 948:174757. https://doi.org/10.1016/j.scitotenv.2024.174757
15. Liu X, Han Y, He F, et al (2021) Characteristic, hazard and iron recovery technology of red mud - a critical review. J Hazard Mater 420:126542. https://doi.org/10.1016/j.jhazmat.2021.126542
16. Swain B, Akcil ,Ata, and Lee J (2022) Red mud valorization an industrial waste circular economy challenge; review over processes and their chemistry. Crit Rev Environ Sci Technol 52:520–570. https://doi.org/10.1080/10643389.2020.1829898
17. Wang H, Liu X, Guan X, et al (2025) Novel high ferrite belite-rich clinker from red mud waste: Hydration mechanism and silicon-containing calcium aluminate hydrate formation. Construction and Building Materials 505:144676. https://doi.org/10.1016/j.conbuildmat.2025.144676
18. Arroyo F, Luna-Galiano Y, Leiva C, et al (2020) Environmental risks and mechanical evaluation of recycling red mud in bricks. Environmental Research 186:109537. https://doi.org/10.1016/j.envres.2020.109537
19. Zhao Y, Liang N, Chen H, Li Y (2020) Preparation and properties of sintering red mud unburned road brick using orthogonal experiments. Constr Build Mater 238:117739. https://doi.org/10.1016/j.conbuildmat.2019.117739
20. Das D, Gołąbiewska A, Rout PK (2024) Geopolymer bricks: The next generation of construction materials for sustainable environment. Constr Build Mater 445:137876. https://doi.org/10.1016/j.conbuildmat.2024.137876
21. Xiao Y, Tiong M, Mo KH, et al (2022) Recycling bayer and sintering red muds in brick production: A review. J Zhejiang Univ-sci A 23:335–357. https://doi.org/10.1631/jzus.a2100476
22. Wang Y, Zhang T, Zhang Y, et al (2019) Transformation and characterization of cement clinker prepared from new structured red mud by sintering. JOM 71:2505–2512. https://doi.org/10.1007/s11837-019-03475-y
23. Jiao H, Yang Y, Yang Y, et al (2026) Red mud as a supplementary cementitious material for low-carbon buildings: Interfacial bonding, structural strength, and environmental benefits. Buildings 16:1717. https://doi.org/10.3390/buildings16091717

24. Wang J, Liu B, Wang D, Sun R (2026) Characterization of red mud and its utilization in preparing alternative cementitious materials: A review. Cleaner Materials 19:100378. https://doi.org/10.1016/j.clema.2026.100378
25. Dixit A, Jain S, Das SK (2024) A systematic characterization of the mixture of red mud and bottom ash as a geomaterial: An efficient utilization in subgrade pavement. J Mater Cycles Waste Manage 26:2159–2174. https://doi.org/10.1007/s10163-024-01955-1
26. Anju MJ, Beulah M, Varghese A (2024) Review of geopolymer composites synthesized using different industrial by-products. Int J Pavement Res Technol. https://doi.org/10.1007/s42947-024-00446-8
27. Bai F, Bai B, Chen J, et al (2024) Development of an ambient cured high-strength red mud-based geopolymer through calcination activation. Sustainable Chemistry and Pharmacy 42:101866. https://doi.org/10.1016/j.scp.2024.101866
28. Guo K, Dong H, Zhang J, et al (2025) Experimental Study of Alkali-Activated Cementitious Materials Using Thermally Activated Red Mud: Effect of the Si/Al Ratio on Fresh and Mechanical Properties. Buildings 15:565. https://doi.org/10.3390/buildings15040565
29. Reddy AS, Iyer KKR, Dave TN (2024) Alkali activated soil stabilization as a sustainable pathway for the development of resilient geotechnical infrastructure. Indian Geotech J 54:945–970. https://doi.org/10.1007/s40098-024-00893-x
30. Fang W, Zhou Y, Cheng M, et al (2024) A review on modified red mud-based materials in removing organic dyes from wastewater:Application, mechanisms and perspectives. J Mol Liq 407:125171. https://doi.org/10.1016/j.molliq.2024.125171
31. Sevgili İ, Dilmaç ÖF, Şimşek B (2021) An environmentally sustainable way for effective water purification by adsorptive red mud cementitious composite cubes modified with bentonite and activated carbon. Separation and Purification Technology 274:119115. https://doi.org/10.1016/j.seppur.2021.119115
32. Liang Z, Peng X, Luan Z (2012) Immobilization of cd, zn and pb in sewage sludge using red mud. Environ Earth Sci 66:1321–1328. https://doi.org/10.1007/s12665-011-1341-0
33. Wang M, Liu X (2020) Applications of red mud as an environmental remediation material: A review. J Hazard Mater 408:124420–124420. https://doi.org/10.1016/j.jhazmat.2020.124420
34. Zhou L, Xu X, Wang Q, et al (2025) Stabilization/solidification of composite heavy metal contaminated soil using a novel red mud-slag based geopolymer (RM-SGP): Performance and mechanisms. Construction and Building Materials 486:141996. https://doi.org/10.1016/j.conbuildmat.2025.141996
35. Suswati D, Denashurya NI (2026) Circular upcycling of bauxite residue (red mud) with cow manure for sustainable forest restoration: Effects on neolamarckia cadamba (roxb.) bosser growth in degraded mine soils. Sustainability 18:5744. https://doi.org/10.3390/su18115744
36. Luo Y, Chen Y, Pan L, et al (2025) Mechanistic insights into organic carbon fraction sequestration in eco-engineered bauxite

residue: Roles of aggregate formation and fe/al oxide interactions. Environmental Research 282:122048. https://doi.org/10.1016/j.envres.2025.122048

37. Cao S, Li J, Nie J, et al (2025) Red mud-based fe/C nanostructured materials for multi-interface remediation of cr(vi)-contaminated soil and stabilization. Environ Sci: Nano 12:1116–1125. https://doi.org/10.1039/d4en01087f
38. Zhou G, Wang Y, Qi T, et al (2023) Toward sustainable green alumina production: A critical review on process discharge reduction from gibbsitic bauxite and large-scale applications of red mud. J Environ Chem Eng 11:109433. https://doi.org/10.1016/j.jece.2023.109433
39. Chandra KS, Krishnaiah S, Reddy NG, et al (2021) Strength development of geopolymer composites made from red mud–fly ash as a subgrade material in road construction. J Hazard Toxic Radioact Waste 25:4020068. https://doi.org/10.1061/(asce)hz.2153-5515.0000575
40. Ma S, Sun Z, Wei J, et al (2022) Utilization of modified red mud waste from the bayer process as subgrade and its performance assessment in a large-sale application. Coatings 12:471. https://doi.org/10.3390/coatings12040471
41. Ma Q, Duan W, Liu X, et al (2022) Engineering performance evaluation of recycled red mud stabilized loessial silt as a sustainable subgrade material. Materials 15:3391. https://doi.org/10.3390/ma15093391
42. Ou X, Chen S, Jiang J, et al (2022) Reuse of red mud and bauxite tailings mud as subgrade materials from the perspective of mechanical properties. Materials 15:1123. https://doi.org/10.3390/ma15031123
43. Parik P, Patra NR (2023) Applicability of clay soil stabilized with red mud, bioenzyme, and red mud–bioenzyme as a subgrade material in pavement. J Hazard Toxic Radioact Waste 27:04023003. https://doi.org/10.1061/JHTRBP.HZENG-1182
44. Wang S, Chen Z, Jiang H, et al (2023) Strength performance and enhancement mechanism of silty sands stabilized with cement, red mud, and phosphogypsum. J Build Eng 73:106762. https://doi.org/10.1016/j.jobe.2023.106762
45. Singh V, Bano S, Chauhan VB, et al (2024) Red mud as a sustainable road construction material: An experimental investigation. Constr Build Mater 411:134549. https://doi.org/10.1016/j.conbuildmat.2023.134549
46. Wang C, Liu H, Wu D, Liu X (2023) Engineering and environmental evaluation of red mud amended volcanic ash as a sustainable subgrade material. Journal of Cleaner Production 393:136353. https://doi.org/10.1016/j.jclepro.2023.136353
47. Kandalai S, Patel A (2025) Geomechanical and microstructural behaviour of expansive soil stabilized with red mud and GGBS: An experimental investigation. Arab J Sci Eng 50:7965–7985. https://doi.org/10.1007/s13369-024-09171-7
48. Silveira NCG, Martins MLF, Bezerra ACS, Araújo FGS (2021) Red mud from the aluminium industry: Production, characteristics, and alternative applications in construction materials—a review. Sustainability 13:12741.

https://doi.org/10.3390/su132212741

49. Mukiza E, Zhang L, Liu X, Zhang N (2019) Utilization of red mud in road base and subgrade materials: A review. Resour Conserv Recycl 141:187–199. https://doi.org/10.1016/j.resconrec.2018.10.031

50. Zhang J, Yao Z, Wang K, et al (2020) Sustainable utilization of bauxite residue (red mud) as a road material in pavements: A critical review. Constr Build Mater 121419. https://doi.org/10.1016/j.conbuildmat.2020.121419

51. Gu J, Liu X, Zhang Z (2023) Road base materials prepared by multi-industrial solid wastes in China: A review. Construction and Building Materials 373:130860. https://doi.org/10.1016/j.conbuildmat.2023.130860

52. Ilahi K, Debbarma S, Mathew G, Inyang HI (2024) Carbon capture and mineralisation using red mud: A systematic review of its principles and applications. Journal of Cleaner Production 473:143458. https://doi.org/10.1016/j.jclepro.2024.143458

53. Patangia J, Saravanan TJ, Kabeer KISA, Bisht K (2023) Study on the utilization of red mud (bauxite waste) as a supplementary cementitious material: Pathway to attaining sustainable development goals. Construction and Building Materials 375:131005. https://doi.org/10.1016/j.conbuildmat.2023.131005

54. Zhang Z, Song Z, Ke G, Dong X (2024) Strengthening mechanism of red mud with calcium oxide. Constr Build Mater 424:135932. https://doi.org/10.1016/j.conbuildmat.2024.135932

55. Tan X (2022) Research on the performance of red mud based semi-flexible pavement (sfp) materials. Doctoral dissertation, Harbin Institute of Technology

56. Peng H (2023) Study on the road usage properties of subgrade fill materials based on modified red mud. Doctoral dissertation, Guizhou University

57. Wan X, Ding J, Wang J, et al (2023) Evolution in macro-micro properties of cement-treated clay with changing ratio of red mud to phosphogypsum. Constr Build Mater 392:131972. https://doi.org/10.1016/j.conbuildmat.2023.131972

58. Zhu Y (2024) Research on the mechanism and application technology of red mud on the bottom base layer and base layer of highway. Doctoral dissertation, Chongqing Jiaotong University

59. Suo C, Wen H, Cao J, et al (2022) Performance of a composite soil prepared with red mud and desulfurized gypsum. KSCE J Civ Eng 26:47–56. https://doi.org/10.1007/s12205-021-2054-x

60. Liu P, Yin S, Zhang X, Huang J (2026) Dynamic characteristics of lime-fly ash-red mud modified silty soil under cyclic traffic loading: a study of hollow cylinder torsional shear. Soil Dynamics and Earthquake Engineering 210:110524. https://doi.org/10.1016/j.soildyn.2026.110524

61. Wu X, Chen Z, Zhou X, et al (2026) Fe-based ternary geopolymer pervious subgrade material: Mechanical performance, reaction mechanism, and sustainability assessment. Processes 14:1607. https://doi.org/10.3390/pr14101607

62. Li W, Huang K, Chen F, et al (2024) Engineering properties and microstructure of soils stabilized by red-mud-based

cementitious material. Materials 17:2340. https://doi.org/10.3390/ma17102340

63. Hu Y, Liang S, Yang J, et al (2019) Role of Fe species in geopolymer synthesized from alkali-thermal pretreated Fe-rich Bayer red mud. Construction and Building Materials 200:398–407. https://doi.org/10.1016/j.conbuildmat.2018.12.122

64. Gu H, Tang M, Wu S, et al (2025) Performance of cementitious composites with bayer red mud as a partial cement replacement. Sci Rep 15:44628. https://doi.org/10.1038/s41598-025-29623-w

65. Wang X, Jing H, Zhang M, et al (2023) Analysis of alkali in bayer red mud: Content and occurrence state in different structures. Sustainability 15:12686. https://doi.org/10.3390/su151712686

66. Ma S, Liu X, Zhang Z, et al (2025) Removal, conversion and utilization technologies of alkali components in bayer red mud. Journal of Environmental Management 373:123781. https://doi.org/10.1016/j.jenvman.2024.123781

67. Yang J, Liu X, Cui K, et al (2025) Hazards and Dealkalization Technology of Red Mud—A Critical Review. Minerals 15:343. https://doi.org/10.3390/min15040343

68. Zhu F, Guo X, Gao H, et al (2024) Ecological restoration affects the dynamic response of alkaline minerals dissolution in bauxite residue. Science of The Total Environment 912:169364. https://doi.org/10.1016/j.scitotenv.2023.169364

69. Lyu F, Hu Y, Wang L, Sun W (2021) Dealkalization processes of bauxite residue: A comprehensive review. Journal of Hazardous Materials 403:123671. https://doi.org/10.1016/j.jhazmat.2020.123671

70. Rai S, Wasewar KL, Agnihotri A (2017) Treatment of alumina refinery waste (red mud) through neutralization techniques: A review. Waste Manag Res: J Int Solid Wastes Public Clean Assoc ISWA 35:563–580. https://doi.org/10.1177/0734242X17696147

71. Chvedov D, Ostap S, Le T (2001) Surface properties of red mud particles from potentiometric titration. Colloids Surf, A 182:131–141. https://doi.org/10.1016/s0927-7757(00)00814-1

72. Kong X, Li M, Xue S, et al (2017) Acid transformation of bauxite residue: Conversion of its alkaline characteristics. Journal of Hazardous Materials 324:382–390. https://doi.org/10.1016/j.jhazmat.2016.10.073

73. Aswathy R, Kumar A (2026) Geotechnical Characterization and Engineering Behaviour of Marine Soil Amended with Industrial Bauxite Residue. Indian Geotech J 1–19. https://doi.org/10.1007/s40098-026-01571-w

74. Wang C, Chen S, Wen B, et al (2025) Red mud modified fly ash based road base materials: Mix design, hydration mechanism, and heavy metal migration behavior. Constr Build Mater 467:140410. https://doi.org/10.1016/j.conbuildmat.2025.140410

75. Hua Y, Heal KV, Friesl-Hanl W (2017) The use of red mud as an immobiliser for metal/metalloid-contaminated soil: a review. Journal of Hazardous Materials 325:17–30. https://doi.org/10.1016/j.jhazmat.2016.11.073

76. Lima MSS, Thives LP, Haritonovs V, Gschoesser F (2020) The influence of alternative fillers on the adhesive properties of

mastics fabricated with red mud. Materials 13:484. https://doi.org/10.3390/ma13020484

77. Wang H, Shi M, Tian X, et al (2023) Experimental study on phosphogypsum-amended red mud as road base material. Sustainability 15:1719. https://doi.org/10.3390/su15021719

78. Sun Z (2018) Research on the engineering technology and environmental impact of bayer red mud filling subgrade. Doctoral dissertation, Shandong University

79. Pratap B, Rao BH, Mondal S, Uniyal K (2026) Treatment methods and influence of red mud and phosphogypsum on pavement composite performance: A state of the art review. Indian Geotech J 56:3220–3248. https://doi.org/10.1007/s40098-025-01460-8

80. Liu P, Yin S, Zheng S, et al (2025) Study on dynamic characteristics of cement-modified red mud-based silty soil under traffic load. Soil Dyn Earthquake Eng 198:109650. https://doi.org/10.1016/j.soildyn.2025.109650

81. James J, Pandian PK (2016) Industrial Wastes as Auxiliary Additives to Cement/Lime Stabilization of Soils. Advances in Civil Engineering 2016:1–17. https://doi.org/10.1155/2016/1267391

82. Romano RCO, Bernardo HM, Maciel MH, et al (2018) Hydration of Portland cement with red mud as mineral addition. J Therm Anal Calorim 131:2477–2490. https://doi.org/10.1007/s10973-017-6794-2

83. Alelweet O, Pavia S, Lei Z (2021) Pozzolanic and Cementing Activity of Raw and Pyro-Processed Saudi Arabian Red Mud (RM) Waste. Recent Prog Mater 03:1–19. https://doi.org/10.21926/rpm.2104047

84. Zhang J, Chen S, Gu F, Wu Y (2023) Industrial waste materials utilized in subgrade modification: A review. China Journal of Highway and Transport 36:1–16. https://doi.org/10.19721/j.cnki.1001-7372.2023.10.001

85. Liu S, Li Z, Li Y, Cao W (2018) Strength properties of bayer red mud stabilized by lime-fly ash using orthogonal experiments. Constr Build Mater 166:554–563. https://doi.org/10.1016/j.conbuildmat.2018.01.186

86. Mukiza E, Liu X, Zhang L, Zhang N (2019) Preparation and characterization of a red mud-based road base material: Strength formation mechanism and leaching characteristics. Construction and Building Materials 220:297–307. https://doi.org/10.1016/j.conbuildmat.2019.06.027

87. Feng L, Yao W, Zheng K, et al (2022) Synergistically using bauxite residue (red mud) and other solid wastes to manufacture eco-friendly cementitious materials. Buildings 12:117. https://doi.org/10.3390/buildings12020117

88. Liu J, Ren F, Ding T, Jia J (2024) Exploring the effect mechanism of Bayer red mud on cement hydration and mechanical properties. Construction and Building Materials 435:136741. https://doi.org/10.1016/j.conbuildmat.2024.136741

89. Silva PB, Ângulo SC, Motta R, Bernucci LLB (2023) Pozzolanic Reaction of Recycled Cementitious and Red Ceramic-Waste Aggregates with Hydrated Lime for Pavement Base Layer. J Mater Civ Eng 35:04022422. https://doi.org/10.1061/(ASCE)MT.1943-5533.0004579

90. Duraisamy S, Chaunsali P (2025) Stabilization of red mud using mineral carbonation. Cleaner Engineering and Technology 25:100926. https://doi.org/10.1016/j.clet.2025.100926
91. Voinea A, Voicu G, Savaniu M, et al (2026) Research on the Utilization of Carbonated Red Mud in Sustainable Construction Materials (Paving Stones). Materials 19:1883. https://doi.org/10.3390/ma19091883
92. Murali Mohan N, Gondu VR, Yamsani SK, Varudu RM (2025) Red mud stabilization using alternate industrial waste materials- mechanical and microstructural properties. Journal of Environmental Management 391:126511. https://doi.org/10.1016/j.jenvman.2025.126511
93. Wang C (2024) Research and application of comprehensive properties of red mud-based stabilized subgrade materials. Doctoral dissertation, Chongqing Jiaotong University
94. Kehagia F (2010) A successful pilot project demonstrating the re-use potential of bauxite residue in embankment construction. Resour Conserv Recycl 54:417–421. https://doi.org/10.1016/j.resconrec.2009.10.001
95. Cheng Y, Jiang N, Wang W, et al (2024) Environment Assessment of Modified Red Mud Utilized in Roadbed. Buildings 14:2135. https://doi.org/10.3390/buildings14072135
96. Shi ML, Tian XT, Wang HJ, et al (2024) Performance of Cement-Lime-Phosphogypsum Solidified Red Mud as Road Base Material. J Chang River Sci Res Inst 41:114. https://doi.org/10.11988/ckyyb.20220847
97. Luo T, Li R, Wei C, et al (2025) Engineering characteristics and environmental impact assessment of modified red mud in subgrade. BULL OF THE CHIN CERAM SOC 44:4633. https://doi.org/10.16552/j.cnki.issn1001-1625.2025.0617
98. Chaudhary M, Saboo N, Gupta A, Miljkovic M (2022) Influence of red mud filler on the fatigue behaviour of bituminous mastic. pp 561–566
99. Liu X, Tang B, Yin H, Emile M (2018) Durability and environmental performance of Bayer red mud-coal gangue-based road base material. Chin J Eng 40:438–445. https://doi.org/10.13374/j.issn2095-9389.2018.04.006
100. Ye Z, Hu N, Chen Y, et al (2026) Synergistic effects of red mud, calcium carbide residue and phosphogypsum for eco-friendly road materials. Journal of Environmental Management 398:128568. https://doi.org/10.1016/j.jenvman.2026.128568
101. Yan L, Yang J, Wu Y, Li F (2026) Research on subgrade construction process based on solidified/stabilized red mud by all-solid-waste binder. J Chang Univ Sci Technol (Nat Sci) 22:23–36. https://doi.org/10.19951/j.cnki.1672-9331.20250221002
102. Chen S, Jiang J, Ou X, Tan Z (2023) Analysis of the synergistic effect on the strength characteristics of modified red mud-based stabilized soil. Materials 16:6104. https://doi.org/10.3390/ma16186104
103. Li Y, Liu X, Li Z, et al (2021) Preparation, characterization and application of red mud, fly ash and desulfurized gypsum based eco-friendly road base materials. J Cleaner Prod 284:124777. https://doi.org/10.1016/j.jclepro.2020.124777
104. Ou X, Zeng Y, Jiang J, et al (2022) Experimental research on the properties of foamed mixture lightweight soil with red mud.

Case Stud Constr Mater 17:e01673. https://doi.org/10.1016/j.cscm.2022.e01673

105. Ma C, Yu T, Zhang N, et al (2024) Study on rheological properties and regulation of bayer red mud-based foamed lightweight soil. Chin J Eng 46:1912–1920. https://doi.org/10.13374/j.issn2095-9389.2023.02.04.003
106. Li P, Liu X, Dong K, Chen C (2025) Red mud and fly ash modified foamed lightweight soil reinforced by fiber for engineering applications: Strength properties and microscopic mechanism. Case Stud Constr Mater 22:e04368. https://doi.org/10.1016/j.cscm.2025.e04368
107. Lin J (2022) Mix proportion design of bayer red mud based foamed lightweight soil and in the application and research of subgrade engineering. Doctoral dissertation, Guangzhou University
108. Hou W, Liu J, Liu Z, et al (2022) Calcium transfer process of cement paste for ettringite formation under different sulfate concentrations. Constr Build Mater 348:128706. https://doi.org/10.1016/j.conbuildmat.2022.128706
109. Wan X, Ding J, Jiao N, et al (2022) Mechanical and microstructural properties of cement-treated marine dredged clay with red mud and phosphogypsum. Bull Eng Geol Environ 81:. https://doi.org/10.1007/s10064-022-02753-5
110. Chen R, Cai G, Dong X, et al (2019) Mechanical properties and micro-mechanism of loess roadbed filling using by-product red mud as a partial alternative. Constr Build Mater 216:188–201. https://doi.org/10.1016/j.conbuildmat.2019.04.254
111. Li X, Sun Z, Wei J, et al (2023) Applicability analysis and performance test of red mud based asphalt powder solidified silt. J Highw Transp Res Dev 40:16-21,28. https://doi.org/10.3969/j.issn.1002-0268.2023.08.003
112. Archambo M, Kawatra SK (2021) Red Mud: Fundamentals and New Avenues for Utilization. Mineral Processing and Extractive Metallurgy Review 42:427–450. https://doi.org/10.1080/08827508.2020.1781109
113. Liu W, Wang S, Zhang T, et al (2025) A Review of Preparation of Low-Carbon Cementitious Materials from Chemically Activated Red Mud: Synergy, Hydration Mechanism, Rheological Properties and Applications. Langmuir 41:15735–15751. https://doi.org/10.1021/acs.langmuir.5c01088
114. Zhu J, Yue H, Ma L, et al (2023) The synergistic hydration mechanism and environmental safety of multiple solid wastes in red mud-based cementitious materials. Environ Sci Pollut Res 30:79241–79257. https://doi.org/10.1007/s11356-023-27800-w
115. Bray AW, Stewart DI, Courtney R, et al (2018) SustainedBauxite residue rehabilitation with gypsumand organic matter 16 years after initial treatment. Environ Sci Technol 52:152–161. https://doi.org/10.1021/acs.est.7b03568
116. Mucsi G, Halyag N, Kurusta T, Kristály F (2021) Control of Carbon Dioxide Sequestration by Mechanical Activation of Red Mud. Waste Biomass Valor 12:6481–6495. https://doi.org/10.1007/s12649-021-01466-2
117. Gomes HI, Mayes WM, Rogerson M, et al (2016) Alkaline residues and the environment: a review of impacts, management practices and opportunities. Journal of Cleaner Production 112:3571–3582. https://doi.org/10.1016/j.jclepro.2015.09.111
118. Sarath Chandra K, Krishnaiah S (2022) Strength and leaching characteristics of red mud (bauxite residue) as a geomaterial in

synergy with fly ash and gypsum. Transportation Research Interdisciplinary Perspectives 13:100566. https://doi.org/https://doi.org/10.1016/j.trip.2022.100566

119. Chen R, Cai G, Congress SSC, et al (2021) Dynamic properties and environmental impact of waste red mud-treated loess under adverse conditions. Bull Eng Geol Environ 80:93–113. https://doi.org/10.1007/s10064-020-01937-1

120. Meshram RB, Mohapatra A, Malakar S, et al (2024) Environmental impact analysis of geopolymer based red mud paving blocks. Discov Appl Sci 6:537. https://doi.org/10.1007/s42452-024-06253-x.

122. Xu H, Zhao F, Hu Y, et al (2024) Cumulative deformation behavior of coarse-grained red mudstone soil under cyclic loading. Int J Geomech 24(11):04024245. https://doi.org/10.1061/IJGNAI.GMENG-9755

123. Liu, H., Wang, C., Wu, D. et al(2025). Deformation properties of red mud-reinforced volcanic ash under long-term cyclic loading. Acta Geotech. 20, 5159 – 5184 . https://doi.org/10.1007/s11440-025-02649-0

121. Dixit A, Das SK (2025) Fly ash stabilised red mud as a one-part alkali-activated sustainable material for pavement subgrade: strength, durability and life cycle assessment analysis. Road Materials and Pavement Design 26:2536–2562. https://doi.org/10.1080/14680629.2025.2454027

List of Captions of Figures and Tables

Figures

Figure 1. Primary aluminium production

Figure 2. Red mud stockpile together with surrounding residential areas and farmlands

Figure 3. Relevant literatures distribution

Figure 4. Schematic diagram of Bayer process production process

Figure 5. Chemical components content of BPRM

Figure 6. Appearance of BPRM (Photo taken at the storage yard of Chalco Zhongzhou Aluminum Co., Ltd.)

Figure 7. BPRM surface “efforescence” phenomenon (photo taken at the storage yard of Henan Baiaoheng New Material Technology Co., Ltd.)

Figure 8. SEM Microscopic morphology of BPRM particles [54] (a) 3000× (b) 20000×

Figure 9. Mechanism of Single Modification of Red Mud Using Traditional Cementitious Materials (a) red mud particles (b) hydration gelation (c) cation exchange (d) carbonation reaction

Figure 10. Strength of cement and lime modified BPRM under different dosages [56][86]

Figure 11. 7 d unconfined compressive strength of cement and lime modified BPRM under different dosages [56]

Figure 12. CBR Expansion Rate of Modified Red Mud [56]

Figure 13. BPRM embankment in Greece (a) initial period of opening to traffic (b) 5 years after opening to traffic [94]

Figure 14. Pavement structure of the demonstration section (a) Jinliqing Expressway (b) Binzhou Beihai venous industrial park [40, 78]

Figure 15. Influence of red mud content on properties of foam lightweight soil (a) flowability (b) unconfined compressive strength [104]

Figure 16. Strength variations with different mass ratio of RM to PG [57]

Figure 17. Unconfined compressive strength of red mud stabilized soil [110]

Figure 18. Mechanism of red mud-cement composite stabilized soil

Figure 19. Schematic diagram of leaching toxicity and groundwater pollution risk of BPRM subgrade

Figure 20. Schematic diagram of leaching test of BPRM subgrade [93]

Tables

Table 1. Main chemical components of BPRM in China

Table 2. Limit moisture content and classification of fine grained soil of BPRM

Table 3. Mechanisms and key products of BPRM modified by cement and lime

1 Table 4. Comparison of cement vs. lime modification of BPRM

2 Table 5. Strength of composition-modified BPRM

3 Table 6. Key findings of composite system

4 Table 7. Leaching toxicity test results of BPRM